การพัฒนาวิธีการตรวจวัดเชิงสี โดยใช้อนุภาคทองขนาดนาโนเมตรเพื่อการวิเคราะห์วิตามินบี 1 และแคลเซียม

DEVELOPMENT OF COLORIMETRIC METHODS USING GOLD NANOPARTICLES FOR

ANALYSIS OF VITAMIN B1 AND CALCIUM

PAWEENAR DUENCHAY

GRADUATE SCHOOL Srinakharinwirot University

2019

การพัฒนาวิธีการตรวจวัดเชิงสี โดยใช้อนุภาคทองขนาดนาโนเมตรเพื่อการวิเคราะห์
วิตามินบี 1 และแคลเซียม

ปวีณา เดือนฉาย

ปริญญานิพนธ์นี้เป็นส่วนหนึ่งของการศึกษาตามหลักสูตร
ปรัชญาดุษฎีบัณฑิต สาขาวิชาเคมีประยุกต์
คณะวิทยาศาสตร์ มหาวิทยาลัยศรีนครินทรวิโรฒ
ปีการศึกษา 2562

DEVELOPMENT OF COLORIMETRIC METHODS USING GOLD

NANOPARTICLES FOR ANALYSIS OF VITAMIN B1 AND CALCIUM

PAWEENAR DUENCHAY

A Dissertation Submitted in partial Fulfillment of Requirements

for DOCTOR OF PHILOSOPHY (Applied Chemistry)

Faculty of Science Srinakharinwirot University

2019

THE DISSERTATION TITLED

DEVELOPMENT OF COLORIMETRIC METHODS USING GOLD NANOPARTICLES FOR ANALYSIS OF VITAMIN B1 AND CALCIUM

BY

PAWEENAR DUENCHAY

HAS BEEN APPROVED BY THE GRADUATE SCHOOL IN PARTIAL FULFILLMENT OF THE

REQUIREMENTS FOR THE DOCTOR OF PHILOSOPHY IN APPLIED CHEMISTRY

AT SRINAKHARINWIROT UNIVERSITY

.... Dean of Graduate School

(Assoc. Prof. Dr. Chatchai Ekpanyaskul, MD.)

....

ORAL DEFENSE COMMITTEE

.... Major-advisor

(Assoc. Prof. Dr.Weena Siangproh)

.... Chair

(Prof. Dr.Orawon Chailapakul)

.... Committee

(Assoc. Prof. Dr.Apinya Chaivisuthangkura)

Title	DEVELOPMENT OF COLORIMETRIC METHODS USING GOLD
	NANOPARTICLES FOR ANALYSIS OF VITAMIN B1 AND CALCIUM
Author	PAWEENAR DUENCHAY
Degree	DOCTOR OF PHILOSOPHY
Academic Year	2019
Thesis Advisor	Associate Professor Dr. Weena Siangproh

This research aimed to develop a colorimetric method using gold nanoparticles for the determination of vitamin B1 and calcium. In the first part, unmodified gold nanoparticles (AuNPs) were used as a colorimetric sensor to determine the quantity of vitamin B1. The specific analysis is based on the aggregation of AuNPs by vitamin B1 due to their ability to form strong electrostatic interactions between positively charged vitamin B1 and negatively charged AuNPs. In the presence of vitamin B1, the distinctive color changes of the AuNPs from red to blue was visualized by the naked eye in ten minutes without the requirement for surface modification. For quantitative measurement using image processing, a good linear relationship (R^2 = 0.9913) between vitamin B1 concentration and average mean red intensity was obtained in the range of 40-200 ppb. The limit of detection (LOD) and the limit of quantitation (LOQ) for vitamin B1 were found to be 3.00 ppb and 10.01 ppb, respectively. The characteristics of developed sensors were investigated for precision, accuracy, sensitivity as well as being validated by the classical method. The statistical analysis proved that the developed sensors were precise, sensitive and accurate and could be used effectively for the analysis of vitamin B1 in urine samples. The second part was concerned with the use of 4-amino-6-hydroxy-2-mercaptopyrimidine monohydrate (AHMP) modified onto gold nanoparticles (AuNPs) for the specification of calcium analysis. Based on the addition of calcium to the AHMP-modified AuNP solution, a color change can be clearly observed by the naked eye within 1 minute, and the color intensity can be measured by Image J software, as a result of the aggregation of AuNPs induced by the electrostatic and binding force between calcium and the modified ligands. The calibration curves of calcium was linear and in the range of 10-100 ppm (R^2 = 0.9877). The limit of detection (LOD) and the limit of quantitation (LOQ) were found to be 3.05 ppm and 10.17 ppm, respectively. Finally, the proposed device was applied for the determination of calcium in urine samples. The results obtained by the developed method were in good agreement with standard AAS results and demonstrated that the proposed method could reliably measure calcium. Overall, this new alternative approach presents a simple, rapid and inexpensive means for the detection of calcium.

Keyword : Vitamin B1, Calcium, Colorimetric method, Gold Nanoparticle, Transparence Sheet-Based Analytical Device

ACKNOWLEDGEMENTS

PAWEENAR DUENCHAY

TABLE OF CONTENTS

LIST OF TABLES

LIST OF FIGURES

CHAPTER I

INTRODUCTION

1. Background

Gold nanoparticles (AuNPs) have been widely used as colorimetric probes for metal ions, anions, small molecules, nucleic acids, and other analyses due to the reason of the unique properties of AuNPs such as optical properties depend on their distances and surface plasmon resonances (Elghanian, Storhoff, Mucic, Letsinger, & Mirkin, 1997). The extinction spectrum and the wavelength of AuNPs at which they absorb and scatter light depends on the distance between particles (Okamoto, Yamaguchi, & Kobayashi, 2000). The unique properties of AuNPs have caused interest for their use in the colorimetric detection. AuNPs have incomplete valence electron on their surfaces, due to the fact that the surface atoms are only bound to the internal atoms (Sethi & Knecht, 2010), (Grasseschi, Zamarion, Araki, & Toma, 2010). This means that the surface atoms can bind to electron acceptor/donor ligands. These would include positively charged ligands, and highly coordinated sulfur and nitrogen groups. This also means that the intermolecular bonds that occur may vary depending on the species binding to the nanoparticles. The binding of analytical compounds to the AuNPs results in changes to the color signal which can be detected by naked eye or Image J program.

Vitamin B1, also known as thiamine, is a water-soluble vitamin. It is an essential nutrient which plays a human role in carbohydrate metabolism, maintenance of neural activity, and prevention of diseases such as nephropathy and beriberi (Lonsdale, 2006). Vitamin B1 consists of an amino-pyrimidine and a thiazole ring linked by a methylene bridge (Kraut J & J, 1962). Human body cannot synthesize vitamin B1 and thus can only obtain from their diet. The Reference Daily Intake (RDI) of vitamin B1 for an adult human is 1.4 mg/day. Clinical signs of vitamin B1 deficiency have been reported when the concentration of vitamin B1 less than 7% of a 1 mg dose that excreted in the urine in a dose retention test (National Research Council [U.S.], 1989) (Council, 1989). For 24-hour urinary excretion, the amount of 0 to 15 Fg of vitamin B1 have been reported for clinical

thiamine deficiency (H.E., 1967). As mentioned, it is therefore of strong interest in the development of a simple (in terms of operation and sensor construction), fast, and reliable method for vitamin B1 detection for biomarker.

Calcium is an essential nutrient and one of the most important mineral for human body. Normally found in the form of salts in human body, the function of calcium is related to the maintenance of bones, teeth, nail and growth (Organization, 1998). Furthermore, in the ionized form, calcium plays a key role in many vital processes such as hormone secretion, nerve conduction and blood coagulation (Group, 1962). World Health Organization (WHO) and Food and Agriculture Organization of the United Nations (FAO) recommended a minimum daily intake of 400–500 mg of calcium (Organization, 1998). At the present, calcium deficiency is taken more seriously. Therefore, in medical diagnostics, the determination of calcium concentration is importance to evaluate a patient's health. A change of the calcium concentration, which usually is relatively stable in body fluids (range in urine: 100 to 300 mg/day) (Carrie, Berg, & Urquhart, 2014), may use to indicate the occurrence of various pathological conditions. When calcium concentrations lower than normal level can indicate osteoporosis, vitamin D deficiency, Eclampsia or hypoparathyroidism whereas the calcium concentrations higher than normal level can indicate hyperparathyroidism, vitamin D intoxication or myeloma (Hyperparathyroidism, 2005). Thus, we should control and often check the calcium concentration from body fluid for protection any disease that would be manifested by an abnormal calcium concentration. Based on previous mentioned, the development of useful device for calcium determination is necessary not only for hypocalcemia but also for hypercalcemia.

From literature reviews, there are many sensing detections for vitamin B1 and calcium such as atomic absorption spectrometry (AAS), spectrofluorimetry (Shankar, & John, 2015), chemiluminescent (M. Kamruzzaman, A.M. Alam, S.H. Lee, & Dang, 2013), electrochemical (Zhou, Tan, Zheng, & Wang, 2013) and fluorescence (RY., 1980), (Lerga, & CK, 2008). However, those mentioned methods need sophisticated

instrument, long analytical period and professional trainers for analysis. In addition, the cost of operation is high.

However, nowadays, the rapid growth of near-patient devices used at home or the hospital bedside are increasing demand for portable systems utilized small disposable sensors for capability of body fluid measurements such as urine sample. In addition, this device should have work by the patients at home within a few minutes by no need instruments to facilitate in daily checkup and reduce cost as well as to save time. Therefore, the conventional methods reported for the determination of vitamin B1 and calcium is limited in use.

Therefore, the objective of this research is to develop cost-effective colorimetric methods using gold nanoparticles for a simple and fast determination of vitamin B1 or calcium in urine samples. The proposed colorimetric sensors are based on the aggregation of pre-concentrated AuNPs induced by vitamin B1 and AHMP-modified AuNPs induced by calcium (II) ions leading to the change of color that can be detected by naked eyes or computer software.

2. Objectives of the research

These research goals were set as following:

2.1 To create a new knowledge of colorimetric analysis that can be used as an alternative way for detection of vitamin B1 and calcium.

2.2 To develop an effectively colorimetric detection of vitamin B1 or calcium in urine sample using gold nanoparticles.

2.3 To apply the developed methods for the analysis of vitamin B1 and calcium in artificial urine sample.

3. Procedures and scope of the research

3.1 Create transparency sheet-based analytical devices

3.2 Prepare pre-concentrated AuNPs

3.3 Optimize conditions for the detection of vitamin B1 such as the AuNPs concentration, the volume ratio between AuNPs and vitamin B1, pH buffer, and incubation time

3.4 Evaluate the performance of developed devices:

3.4.1 Linear relationship between the intensity of color and concentration of vitamin B1

3.4.2 Limit of detection (LOD) for vitamin B1 analysis

3.4.3 Limit of quantitation (LOQ) for vitamin B1 analysis

3.5 Detect vitamin B1 in artificial urine sample and validate developed device using the traditional method such as spectrofluorometry

3.6 Study the modification of AuNPs surface with 4-Amino-6-hydroxy-2-mercaptopyrimidine monohydrate (AHMP) for the detection of calcium

3.7 Optimize conditions for the detection of calcium including the modifier volume ratio, pH buffer, incubation time, and reagent ratio

3.8 Evaluate the performance of developed devices:

3.8.1 Linear relationship between the intensity of color and concentration of calcium

3.8.2 Limit of detection (LOD) for calcium analysis

3.8.3 Limit of quantitation (LOQ) for calcium analysis

3.9 Detect calcium in artificial urine sample and validate developed device by using the standard atomic absorption spectroscopic method

4. Expected benefits

4.1 To obtain a new knowledge of colorimetric analysis using gold nanoparticles for detection of vitamin B1 and calcium in urine sample

4.2 To obtain a prototype for the detection of vitamin B1 and calcium using transparency sheet-based devices for use as an alternative detection of vitamin B1 or calcium in urine sample with accuracy, cost effectiveness, and easy to use

CHAPTER II

THEORY AND LITERATURE REVIEW

1. Colorimetric method

Colorimetric method is a technique used to determine the concentration of colored compounds in solution. A colorimeter is a device used to monitor the concentration of a solution by measuring its absorbance at a specific wavelength of light. The measure of color is a convenient method of quantitative determination of materials which is itself colored or can be reacted to produce a color. Variation of the color intensity with changes in concentration of colored component is the basis of colorimetric analysis. Therefore, calorimetric analysis is concerned with determination of the concentration of a substance based on relative absorption of light with respect to a known concentration of a substance. In a colorimetric chemical test the intensity of the color from the reaction must be proportional to the concentration of the substance being tested.

A colorimeter is generally any tool that characterizes colored samples to provide an objective to measure of color characteristics. In chemistry, the colorimeter is an apparatus that allows the absorbance of a solution at a particular frequency (color) of visual light to be determined. Colorimeters hence make it possible to ascertain the concentration of a known solute, since its color is proportional to the absorbance. Global Water's colorimeters pass a colored light beam through an optical filter, which transmits only one particular color or band of wavelengths of light to the colorimeter's photo detector where it is measured. The difference in the amount of monochromatic light transmitted through a colorless sample (blank) and the amount of monochromatic light transmitted through a test sample is a measurement of the amount of monochromatic light absorbed by the sample. In most colorimetric tests the amount of monochromatic light absorbed is directly proportional to the concentration of the test factor producing the color and the path length through the sample (Figure 1). However, for a few tests the relationship is reversed and the amount of monochromatic light absorbed is inversely

proportional to the concentration of the test factor. The choice of the correct wavelength for testing is important. It is interesting to note that the wavelength that gives the most sensitivity (lower detection limit) for a test factor is the complementary color of the test sample. For example, the Nitrate-Nitrogen test produces a pink color proportional to the nitrate concentration in the sample (the greater the nitrate concentration, the darker the pink color). A wavelength in the green region should be selected to analyze this sample since a pinkish-red solution absorbs mostly green light (Armbrecht, 2011), (P., 2000).
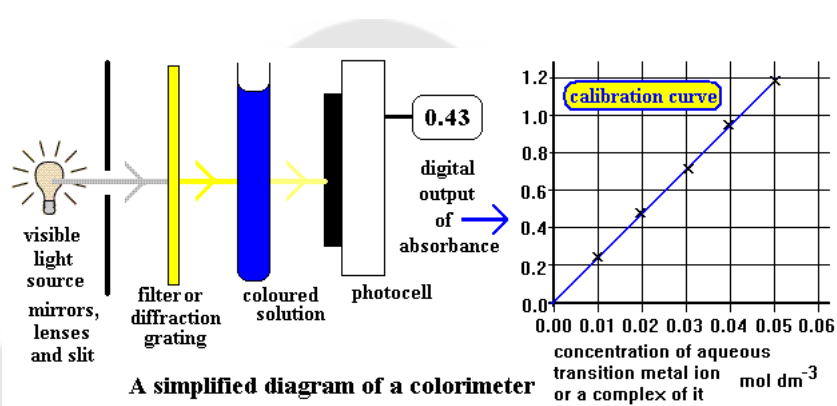
Figure 1 Diagram of a colorimeter.

From: Brown, Z.P. (2000) "Colorimetry-Quantitative Analysis and Determining the Formula of a Complex ion" Retrieved 28 January 2019, from http://www.docbrown.info/page07/appendixtrans09.

2. Nanoparticles

Nanoparticle is a small substance that behaves as a whole unit in terms of its transport and properties. All physical and chemical properties are size dependent, and the properties of materials on the nano-size scale have important consequences in wide ranging fields. Nanoparticles have different property from atomic ones or nano-clusters as well as different from bulk particles. Thus, nanoparticles can be defined as entities measuring from 1 to 10 nm and built of atoms of one or several elements (Table 1). Nanoparticles may or may not exhibit size-related properties that are seen in fine

particles. The characteristics of nanoparticles especially depend on their composition, size and size distribution, shape and morphology, their specific surface area and charge as well as their chemical surface modification. Surface Plasmon resonance (SPR) is a prominent spectroscopic feature of noble metal nanoparticles (NPs) for measuring the refractive index of very thin layers of material adsorbed on metal. A fraction of the light energy incident at a sharply defined angle can interact with the delocalized electrons in the metal film thus reduction the reflected light intensity (Sergeev, & Shabatina, 2002), (Homola, Yee, & Gauglitz, 1999).
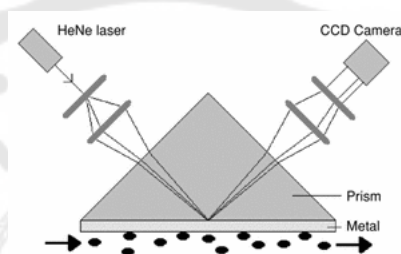
Figure 2 The most common geometrical setup of SPR. The incoming light is located on the opposite side of the metallic slab than the adsorbate.

From: Homola, J., et al. (1999). "Surface Plasmon Resonance Sensors: Review." Sensors and Actuators B 54(1-2): 3-15.

Table 1 Classification of particles by size.

Chemistry	Nanoparticles	Solid-state physics
Atom	$N = 10 - 10^4$	$N = 10^4$- Bulk Matter
Diameter (nm)	$1 - 10$	> 100

From: Sergeev G.B., Shabatina T.I. (2002)." Low temperature. Surface chemistry and nanostructures." Surf. Sci. 500: 628-655.

2.1 Gold nanoparticles (GNPs)

Colloidal gold nanoparticles have been utilized for centuries by artists due to the vibrant colors produced by their interaction with visible light. The shape and size dependence of the absorption wavelength is such that the color of the particles depends on their preparation, with larger particles and more asymmetric particles absorbing, more spherical, particles. The longer wavelengths correspond to lower frequencies, which mean that the electrons in a bigger box oscillate with a lower frequency than those in a smaller box. Gold nanoparticles interaction with light is strongly dictated by their environment, size and physical dimensions. Oscillating electric fields of a light ray propagating near a colloidal nanoparticle interact with the free electrons causing a concerted oscillation of electron charge that is in resonance with the frequency of visible light. These resonant oscillations are known as surface plasmons. For small (~30nm) monodispersed gold nanoparticles, the surface plasmon resonance phenomena causes an absorption of light in the blue-green portion of the spectrum (~450 nm) while red light (~700 nm) is reflected, yielding a rich red color. As particle size increases, the wavelength of surface plasmon resonance related absorption shifts to longer wavelengths. Red light is then absorbed, and blue light is reflected, yielding solutions with a pale blue or purple color (Figure 3). As particle size continues to increase toward the bulk limit, surface plasmon resonance wavelengths move into the IR portion of the spectrum and most visible wavelengths are reflected, giving the nanoparticles clear or translucent color. The surface plasmon resonance can be tuned by varying the size or shape of the nanoparticles, leading to particles with tailored optical properties for different applications (Hinterwirth et al., 2013).
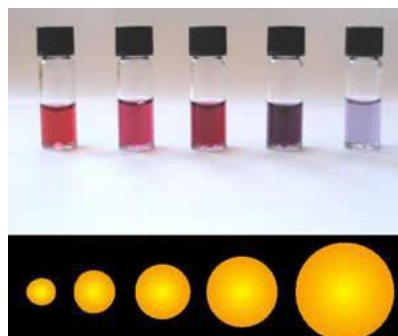
Figure 3 Colors of various sized monodispersed gold nanoparticles.

From: Bara, M., (2015). "Gold nanoparticles for determination of biomolecules."
Retrieved 23 march 2018, from http://www.slideshare.net/Albairaq/presentation-al-bairaq-repaired.

This phenomenon is also seen when excess salt is added to the gold nanoparticle solution. The surface charge of the gold nanoparticle becomes neutral, causing the aggregation of nanoparticles. As a result, the solution color changes from red to blue. To minimize aggregation, the versatile surface chemistry of gold nanoparticles allows them to be coated with polymers, small molecules, and biological recognition molecules. This surface modification enables gold nanoparticles to be used extensively in chemical, biological, engineering, and medical applications.

2.2 Modified surface of gold nanoparticles (modified-AuNPs)

The modification of the surface of nanoparticles is an important and challenge because metal nanoparticles possess unique features compared to equivalent larger-scale materials and it is necessary to stabilize or functionalize. The method for surface modification of AuNPs with small molecules was developed and used in bio-sensing applications; the bio macromolecules such as antibody, enzyme or polysaccharide. Moreover, the orientation and accessibility of those small molecules can be controlled without their bioactivity's accommodation, so the small molecules functionalized AuNPs could be high favorable for the stability and repeatability in detection of biochemical

assays. Since the surface chemistry of AuNPs is significant to biochemical assays, it is important to summarize the strategies for surface modification of AuNPs with small molecules. Thus, this recent progress was focused on the surface chemistry for functionalization of AuNPs with small molecules including click chemistry, ligand exchange strategy, and coordination-based recognition (Chen, Xianyu, & Jiang, 2017).

The literature on modification of metal nanoparticles is very numerous with gold nanoparticles. The applications were found in the various researches, such as catalysis, chemical sensing, bio-labeling or photonics. Bio-applications of gold nanoparticles are popular used because of a good oxidation resistance, easy synthesis and optical properties. The metal nanoparticles were modified by other compounds that will be provided in following sections.

For thiols and disulfides, the organosulfur compounds can modify onto metal nanoparticles because organosulfur groups strongly coordinate to various metals, such as Ag, Cu, Pt, Hg, Fe, or Au. Sulfur possesses a huge affinity for metal surfaces. Moreover, interaction between the metal and sulfur is also sufficiently strong to immobilize the thiol groups on the surface of metal nanoparticles. However, when the thiol function is oxidized to sulfate or sulfonate, the interaction with gold will decrease. Thiol- or disulfide-capped nanoparticles can be prepared by two methods. First, sulfur compounds were grafted on the surface of resynthesized nanoparticles covered by solvent molecules which will be replaced by the sulfur containing ligands.

The second is synthesis of an organosulfur-capped nanoparticle in a one-step process, where the metal precursor and the protective ligand are reacted simultaneously. In this case, two processes compete with each other. Chemisorption of thiols on the metal surface occurs with concomitant cleavage of the S–H bond. For carboxylic acids, the metal surfaces interact with negatively charged carboxylate groups by deprotonation of carboxylic acids.

For phosphines, the gold nanoparticles were protected by triphenylphosphine after modification with phosphine. The phosphine interaction with the metal nanoparticle is very weak and thus results in a very poor stability of the nanoparticles. The lack of

stability results in an easy exchange with other ligands, which are more strongly bonded to the metal surface such as the thiol exchange and amine exchange.

And for amines and ammonium ions, it is generally applied to stabilize the particles. The Pd nanoparticles modified with hexadecylamine leads to a better dispersion and stability of the particles. The interaction between amino groups and metal nanoparticle surfaces is much weaker than thiol groups because the amine-modified nanoparticles are bigger and weaker than organosulfur-modified. Nevertheless, ammonium ions, having shorter chain lengths of 4–8 carbons, have also been used to stabilize transition metal nanoparticles. When the metal nanoparticles were synthesized electrochemically, the ammonium surfactant will serve as electrolytes stabilizer (Neouze & Schubert, 2008).

3. The techniques used for characterization and validation

Sizes and physicochemical properties of nanoparticles are closely interrelated and importance for studying their chemical transformations. Furthermore, there are different approaches to study the properties of the particles on the surface and in the bulk. The main techniques used for determining sizes and certain properties of nanoparticles in the liquid phase are as follows:

3.1 Ultraviolet–Visible Spectroscopy (UV-Vis)

Many molecules absorb ultraviolet or visible light. The absorbance of a solution increases as attenuation of the beam increases. If matter is exposed to electromagnetic radiation, e.g. infrared light, the radiation can be absorbed, transmitted, reflected, scattered or undergo photoluminescence (Subodh, 2006). Photoluminescence is a term used to designate a number of effects, including fluorescence, phosphorescence, and Raman scattering (Figure 4).
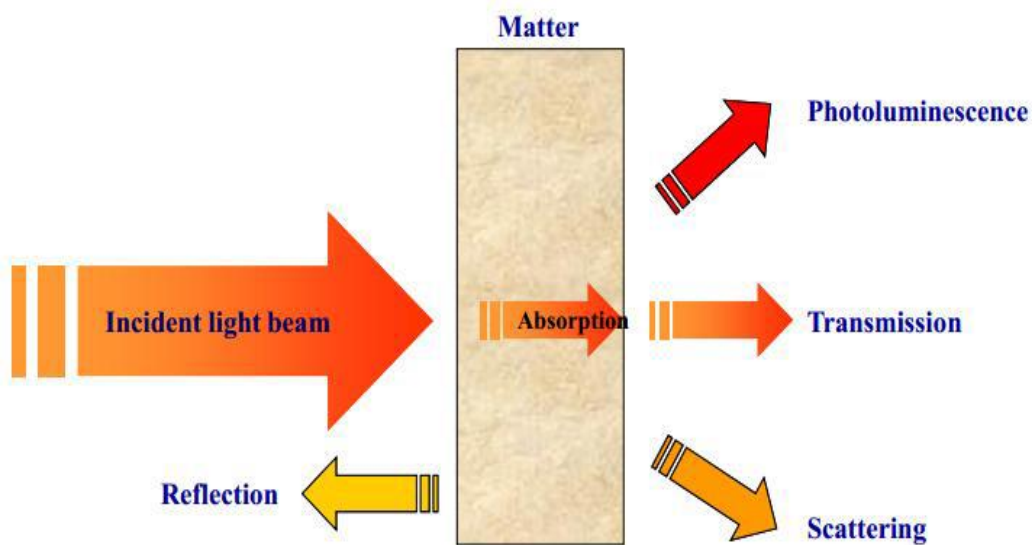
Figure 4 Phenomenon that occurs when light travels through the cuvette.

From: Penner, M.H., (2010). "Basic Principles of Spectroscopy" Food analysis, Fourth Edition, Springer: 375-385.
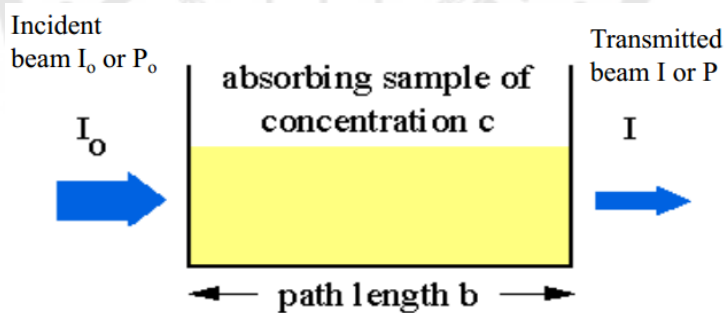
Figure 5 Absorption of light by a sample.

From: Clark, J., (2015). "The Beer-Lambert Law". Retrieved 23 march 2018, from http://chemwiki.ucdavis.edu/Core/Physical_Chemistry/Spectroscopy/Electronic_Spectro scopy/Electronic_Spectroscopy_Basics/The_Beer-Lambert_Law.

Absorbance is directly proportional to the path length, b, and the concentration, c, of the absorbing species as shown in Figure 5. Beer-Lambert Law (also known as Beer's Law) states that here is a linear relationship between the absorbance and the concentration of a sample (Apilux et al., 2010). Beer's Law can only be applied when there is a linear relationship. The method is most often used in a quantitative way to determine concentrations of an absorbing species in solution.

$$A = \log \frac{I_o}{I} = \varepsilon bc$$

Where : A = Absorbance

I_0 = Intensity of the incident light

I = Intensity of the light transmitted through the sample

ε = Molar absorptivity (L mol^{-1}cm^{-1})

b = sample path length (cm)

c = Concentration of the solution (mol/L)

Different molecules absorb radiation of different wavelengths. An absorption spectrum will show a number of absorption bands corresponding to structural groups within the molecule. This absorption spectroscopy uses electromagnetic radiations between 190 nm to 800 nm and is divided into the ultraviolet (UV, 190-400 nm) and visible (VIS, 400-800 nm) regions (Table 2). Since the absorption of ultraviolet or visible radiation by a molecule leads transition among electronic energy levels of the molecule, it is also often called as electronic spectroscopy. The information provided by this spectroscopy when combined with the information provided by NMR and IR spectral data leads to valuable structural proposals (Figure 6).

A

Diffraction Grating

Light source

Monochromator

Sample

Detector

B

Diffraction Grating

Light source

Monochromator

Mirror

Mirror

Reference

Detector

Sample

Detector
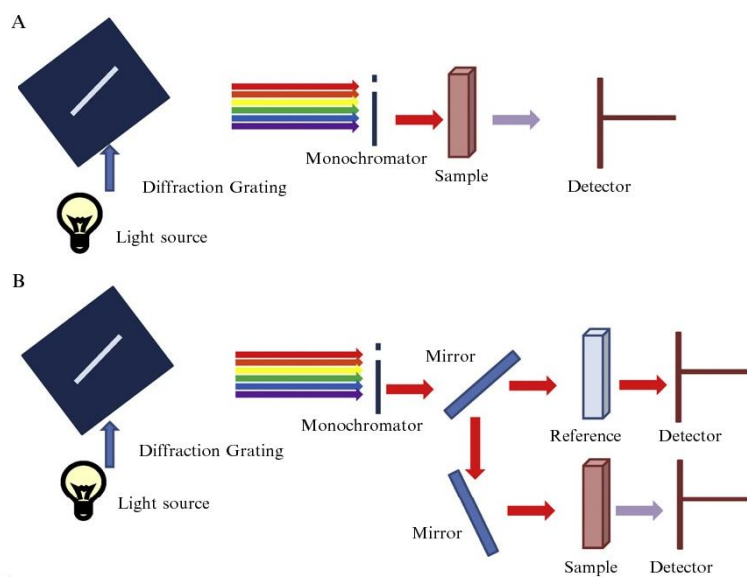
Figure 6 Basic Instrumentation of the spectrophotometer: (A) single beam and (B) double Beam.

From: Nilapwar, S.M., (2011). "Absorption spectroscopy Methods." Enzymol 500:59-75. doi: 10.1016/B978-0-12-385118-5.00004-9.

Table 2 Relationships between light absorption and color.

Wavelength Absorbed (nm)	Absorbed Color	Transmitted Color (Complement)
380-450	Violet	Yellow-green
450-495	Blue	Yellow
495-570	Green	Violet
570-590	Yellow	Blue
590-620	Orange	Green-blue
620-750	Red	Blue-green

From: Penner, M.H. (2010). "Basic Principles of Spectroscopy", Food analysis, Fourth Edition, Springer: 375-385.

3.2 Zeta potential

Zeta potential analysis is a technique for determining the surface charge of nanoparticles in solution (colloids). Nanoparticles have a surface charge that attracts a thin layer of ions of opposite charge to the nanoparticle surface. This double layer of ions travels with the nanoparticle as it diffuses throughout the solution (Figure 7). The electric potential at the boundary of the double layer is known as the Zeta potential of the particles and has values that typically range from +100 mV to -100 mV. The magnitude of the zeta potential is predictive of the colloidal stability. Nanoparticles with Zeta potential values greater than +25 mV or less than -25 mV typically have high degrees of stability. Dispersions with a low zeta potential value will eventually aggregate due to Van Der Waal inter-particle attractions. Zeta potential is an important parameter for understanding the state of the nanoparticle surface and predicting the long-term stability of the nanoparticle. Therefore, Zeta -potential analysis can use to determine a successfulness fora surface modification or monitoring a processing step of modified the nanoparticle surface (Nanocomposix, 2012).
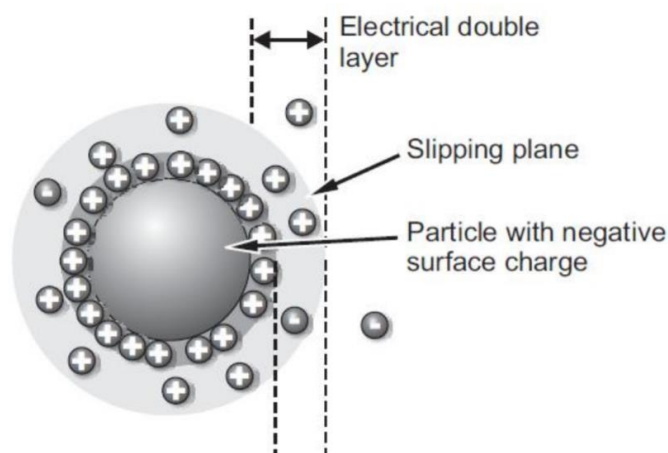
Figure 7 Electric double layer surrounding nanoparticles.

From: Zeta potential analysis of nanoparticals September 2012, V 1.1 4878 Ronson CT STE K Sandiego, CA 92111 858 - 565 – 4227, Nanocomposix.com.

Particle size distributions were measuring by the angular variation in intensity of light scattered as a laser beam passes through a dispersed particulate sample. Large particles scatter light at small angles relative to the laser beam and small particles scatter light at large angles, as illustrated below (Figure 8). The angular scattering intensity data is then analyzed to calculate the size of the particles responsible for creating the scattering pattern, using the Mie theory of light scattering. The particle size is reported as a volume equivalent sphere diameter. It is commonly present this distribution in the form of either a frequency distribution curve, or a cumulative (undersize) distribution curve.
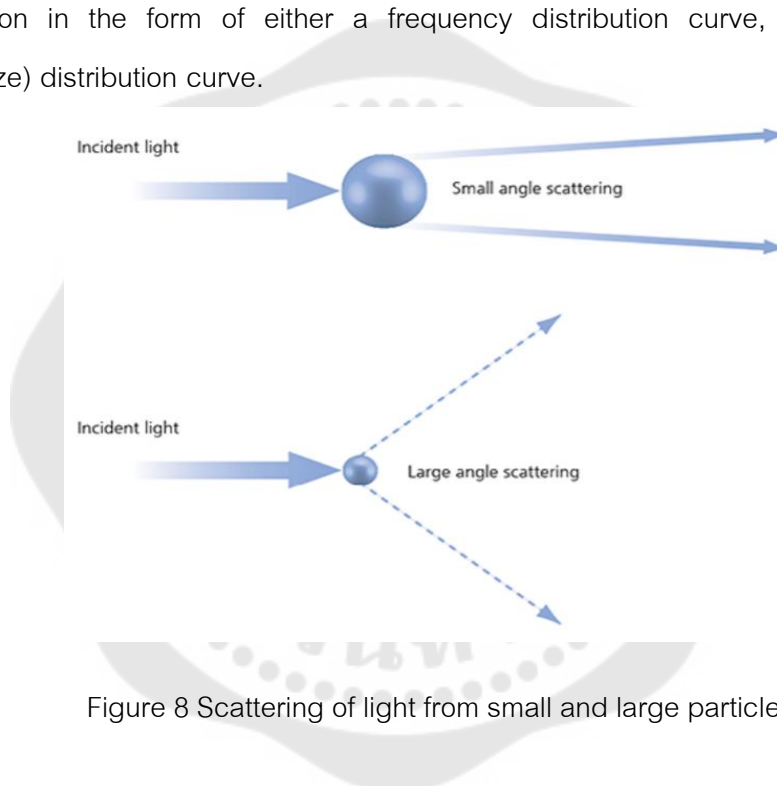
Figure 8 Scattering of light from small and large particles.

From: Zeta potential analysis of nanoparticals September 2012, V 1.1 4878 Ronson CT
STE K Sandiego, CA 92111 858 - 565 – 4227, Nanocomposix.com.

3.3 Fluorescence spectroscopy

Fluorescence is one of analytical method for analysis the molecules that are excited by irradiation at a certain wavelength and emit radiation of a different wavelength. The emission spectrum provides information for both qualitative and quantitative analysis. Many publications have mentioned the use of derivatization reactions in the analysis of vitamin B1. Vitamin B1 and its esterified derivatives are

transformed into thiochrome derivatives by alkaline oxidation. Many of the derivatization reagents including potassiumferricyanide ($K_3Fe(CN)_6$), cyanogen bromide (BrCN) or mercuricchloride ($HgCl_2$) are routinely used as oxidation reagents as shown in Figure 9. The reaction product exhibits strong fluorescence in the emission region of 420–445 nm, after subsequent excitation with 360–375 nm light. The reaction is simple, rather specific and increases the sensitivity, enabling quantitative analysis even in the nmoL to pmol/L region. Stability of thiochrome derivatives is often discussed. Some publications have noted the stability of thiochrome. They claimed that after 48 h there has no decomposition or loss in detectability (Lu & Frank, 2008), (Ito, Yamanaka, Susaki, & Igata, 2012). Derivatization in chromatographic systems can be performed pre-column or post-column depending on the desired conditions, equipment or type of preparation used (Liddicoat, Hucker, Liang, & Vriesekoop, 2015).
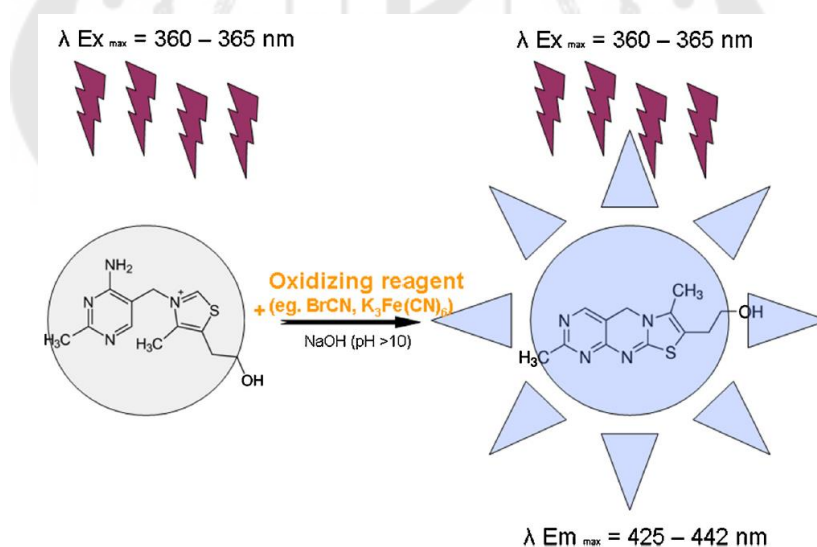
Figure 9 Diagram of a derivatization reaction of vitamin B1 that produces a highly fluorescent thiochrome derivative.

From: Jaroslav, J., et al., (2017). "Recent trends in determination of thiamine and its derivatives in clinical practice." Journal of Chromatography A 1510: 1–12.

3.4 Atomic Absorption Spectroscopy (AAS)

Atomic absorption spectrometry (AAS) is a technique for measuring quantities of chemical elements presented in environmental samples by measuring the absorbed radiation by the chemical element of interest. This is performed by reading the spectra produced when the sample is excited by radiation. The atoms absorb ultraviolet or visible light and make transitions to higher energy levels. Atomic absorption methods measure the amount of energy in the form of photons of light that are absorbed by the sample. A detector measures the wavelengths and intensity of light transmitted by the sample, and compares them to the wavelengths and intensity which originally passed through the sample. A signal processor then integrates the changes in wavelength absorbed, which appear in the readout as peaks of energy absorption at discrete wavelengths. The energy required for an electron to leave an atom is known as ionization energy and is specific to each chemical element. When an electron moves from one energy level to another within the atom, a photon is emitted with energy (E). Atoms of an element emit a characteristic spectral line. Every atom has its own distinct pattern of wavelengths at which it will absorb energy, due to the unique configuration of electrons in its outer shell. This enables the qualitative analysis of a sample. The concentration is calculated based on the Beer-Lambert law. Absorbance is directly proportional to the concentration of the analyte absorbed for the existing set of optimal conditions. The concentration is usually determined from a calibration curve, obtained using standards of known concentration. However, applying the Beer-Lambert law directly in AAS is difficult due to variations in atomization efficiency from the sample matrix, non-uniformity of concentration and path length of analyte atoms (Havezov, 1996).

4. Vitamin B1

Vitamin B1 (Thiamine) is a water-soluble vitamin with reduced solubility in alcohols and negligible solubility in less polar organic solvents (Edwards et al., 2017). Commercially, it is available in the form of thiamine hydrochloride or thiamine mononitrate (Edwards et al., 2017), (Macek, Feller, & Hanus, 1950). Structurally, vitamin

B1 consists of 2-methyl-4-aminopyrimidine attached via a methylene group to a thiazole ring substituted with a methyl group in the fourth position and a hydroxyethyl group in the fifth position. The human body is unable to synthesize vitamin B1. Its concentration relies entirely on dietary intake and the composition of nutrients and beverages. After ingestion, dietary vitamin B1 is extensively converted to free thiamine, which then can be absorbed in the digestive tract by active or passive transport depending on the intake level (Batifoulier, Verny, Besson, Demigne, & Remesy, 2005). Thiamine diphosphate (ThDP) is the most abundant biologically active form in the human body and creates approximately 80% of the total thiamine content. It is mainly found in leukocytes and erythrocytes, while plasma mainly contains free thiamine and its monophosphateester (ThMP). All of the excess thiamine content and its degradation products can be found in urine (Losa, Sierra, Fernandez, Blanco, & Buesa, 2005). After starvation of vitamin B1 in the diet, the excessive intake of thiaminase rich foods or due to some pathophysiological processes, body stores can be reduced within 2 weeks and vitamin B1 deficiency can develop (Ahmed, Azizi-Namini, Yan, & Keith, 2015). Deficiency of vitamin B1 results in a whole set of conditions, mostly due to impaired cellular metabolic function and oxidative stress that may be manifested as Beriberi (Abdou & Hazell, 2015). Various causes can reduce the level of vitamin B1, such as alcoholism (Allison & McCurdy, 2014), diabetes (Waheed, Naveed, & Ahmed, 2013), interactions with antibiotics (McCabe, 2004), unbalanced diet (Kerns, Arundel, & Chawla, 2015), inflammatory processes (Densupsoontorn, Jirapinyo, & Kangwanpornsiri, 2013), and some oncological diagnoses (Lee, Yanamandra, & Bocchini, 2005). Therefore, the monitoring levels of vitamin B1 and its metabolites in these groups of patients, especially patients hospitalized in intensive care have been paid attention.
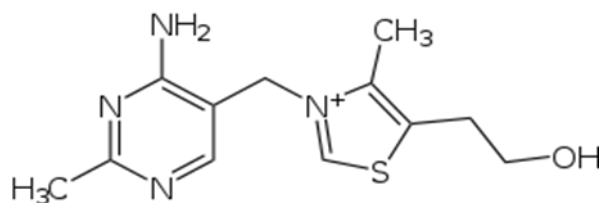
Figure 10 Structure of vitamin B1.

From: Ramar, R.; & Malaichamy, I. (2017). "Simple and visual approach for highly selective sensing of vitamin B1 based on glutathione coated silver nanoparticles as a colorimetric prob." Sensors and Actuators B 244: 380-386

5. Calcium

Calcium is an essential nutrient and one of the most mineral for vital body. It is well-known for its key role in bone health. Calcium also helps maintain heart rhythm, muscle function, and many vital processes such as hormone secretion, nerve conduction and blood coagulation (Gafni et al., 2015). The Institute of Medicine has set Dietary Reference Intakes (DRI) and Recommended Daily Allowances (RDA) for calcium. It is 1,000 – 1,500 mg/day for infants, 2,500 mg/day for children, 3,000 mg/day for teens, 2,500 mg/day for adults 19-50 years, and 2,000 mg/day for adults over the age of 51 years (Organization, 1998). At the present, calcium deficiency is taken more seriously. Many people are an increased risk for calcium deficiency. This deficiency may be due to a variety of factors, including poor calcium intake over a long period of time, medications that may decrease calcium absorption, dietary intolerance to foods rich in calcium, hormonal changes, and certain genetic factors.

Then in clinical diagnostics, the determinations of calcium concentration are importance to evaluation a patient's health. A change of the calcium concentration, which usually is relatively stable in body fluids (range in urine: 100 to 300 mg/day) (Carrie E. Black et al., 2014). These may indicate the presence of various pathological conditions. When calcium concentrations lower than normal level may indicated

osteoporosis, vitamin D deficiency, eclampsia or hypoparathyroidism whereas the calcium concentrations higher than normal level may indicated hyperparathyroidism, vitamin D intoxication or myeloma (Hyperparathyroidism, 2005). Thus, we should control and often check the calcium concentration from body fluid for protection any disease that would be manifested by an abnormal calcium concentration. The device for calcium determination must be necessary for deficiency screening.

6. Image J

Image J is a public domain Java image processing and analysis program inspired by NIH Image for the Macintosh. It runs, either as an online applet or as a downloadable application, on any computer with a Java 1.5 or later virtual machine. Downloadable distributions are available for Windows, Mac OS X and Linux. It can display, edit, analyze, process, save and print 8–bit, 16–bit and 32–bit images. It can read many image formats including TIFF, GIF, JPEG, BMP, DICOM, FITS and 'raw'. It supports 'stacks' (and hyper stacks), a series of images that share a single window. It is multithreaded, so time-consuming operations such as image file reading can be performed in parallel with other operations1. It can calculate area and pixel value statistics of user-defined selections. It can measure distances and angles. It can create density histograms and line profile plots. It supports standard image processing functions such as contrast manipulation, sharpening, smoothing, edge detection and median filtering. It does geometric transformations such as scaling, rotation and flips. Image can be zoomed up to 32:1 and down to 1:32. All analysis and processing functions are available at any magnification factor. The program supports any number of windows (images) simultaneously, limited only by available memory. Spatial calibration is available to provide real world dimensional measurements in units such as millimeters. Density or gray scale calibration is also available. Image J was designed with an open architecture that provides extensibility via Java plugins. Custom acquisition, analysis and processing plugins can be developed using Image J's built in editor and Java compiler. User-written plugins make it possible to solve almost any image processing or

analysis problem. Being public domain open source software, an Image J user has the four essential freedoms defined by the Richard Stallman in 1986: 1) The freedom to run the program, for any purpose; 2) The freedom to study how the program works, and change it to make it do what you wish; 3) The freedom to redistribute copies so you can help your neighbor; 4) The freedom to improve the program, and release your improvements to the public, so that the whole community benefits. Image J is being developed on Mac OS X using its built-in editor and Java compiler, plus the BBEdit editor and the Ant build tool. The source code is freely available. The author, Wayne Rasband (wsr@nih.gov), is a Special Volunteer at the National Institute of Mental Health, Bethesda, Maryland, USA (T. & W., 2012).

7. Literature Reviews

Currently, there are many sensing detections for vitamin B1 and calcium such as atomic absorption spectrometry (AAS), spectrofluorimetry (Shankar, & John, 2015), chemiluminescent (M. Kamruzzaman, A.M. Alam, S.H. Lee, & Dang, 2013), electrochemical (Zhou, Tan, Zheng, & Wang, 2013) and fluorescence (RY., 1980), (Lerga, & CK, 2008). Because of biomarkers are interesting and growing in paid attention for analytical chemistry. It is a tool for detected disease in the early stage.

7.1 Literature review for the analytical vitamin B1

In 2017, Ramar and Malaichamy (Ramar & Malaichamy, 2017) reported a colorimetric method detection of vitamin B1 by silver nanoparticles (AgNPs). AgNPs surface was modified by glutathione (GSH). The sensitivity of colorimetric assay is based on the surface plasmon resonance band (SPR) changes and aggregation of glutathione modified AgNPs (GSH-AgNPs) upon the addition of vitamin B1. The selectivity of GSH-AgNPs based determination of vitamin B1 is excellent, compared with other relevant vitamin interferences. GSH-AgNPs identified for the detection of vitamin B1, it caused by their ability to strong electrostatic interaction between positively charged vitamin B1 and negatively charged GSH coated AgNPs. This spectral and visual colorimetric approach show a highly sensitivity for vitamin B1 with a detection limit

50.00×10^{-9} mol dm^{-3}. The colorimetric assay was effectively applied to the detection of vitamin B1 in spiked human blood serum and urine samples.

In 2016, María Ángeles and co-workers (María Ángeles, Aguilar-Caballos, & Gómez-Hens, 2016) described a photometric method for the determination of free and total vitamin B1 in food samples. This method is based on the use of gold nanoparticles (AuNPs) which aggregate in the presence of vitamin B1 owing to the interaction of its sulfur atom with the AuNPs. This is accompanied by a color change from wine red to purple-blue and an increase in absorbance at 590 nm. The effect is not observed for thiamin phosphates which, however, can be determined, as demonstrated for the example of thiamin pyrophosphate as a model ester, by treating them with alkaline phosphatase (ALP) which hydrolyses such esters. The use of two sample aliquots, one with and one without ALP, allows the determination of free and total thiamin, respectively. The linear range extends from 0.15 to 3.5 μM, and the detection limit is 54 nM of vitamin B1. The method has been applied to the analysis of spiked food samples and gave recoveries that ranged between 88.8 and 100.7 %.

In 2016, Sulafa and co-workers (Sulafa, Elbashir, El-Mukhtar, & Ibrahim, 2016) presented a spectrophotometric determination of vitamin B1 in pharmaceutical tablets. The proposed method is based on the reaction of vitamin B1 and 7-Chloro-4-nitrobenzoxadiazole (NBD-Cl) at alkaline medium to develop a deep brown adduct that bear maximum absorption at 434 nm. Under optimized reaction conditions, the limit of detection (LOD) and limit of quantification (LOQ) were found to be 0.667 μg/ml and 2.020 μg/ml respectively. The method has been successfully applied to the determination of vitamin B1 in pharmaceutical formulations, and can be used as an alternative of the existing sophisticated method used in drug laboratories and factories.

In 2015, Shankar and John (Shankar & John, 2015) detected vitamin B1 using 4-amino-6-hydroxy-2-mercaptopyrimidine capped gold nanoparticles (AHMP-AuNPs) by spectrofluorimetry. The emission intensity of AHMP-AuNPs was enhanced even in the presence of picomolar concentration of vitamin B1. Based on the enhancement of emission intensity, the concentration of vitamin B1 was determined. The present

fluorophore showed an extreme selectivity towards the determination of vitamin B1 in the presence of 10,000-fold common interferents including vitamin B2, B3, B6, B9 and vitamin C while the presence of cysteine and glutathionine interferes for the determination of vitamin B1. A good linearity was observed from 10 to 120 x 10^{-12} M vitamin B1 and a detection limit was found to be 6.8 fML^{-1}. The present method was successfully used for the determination of vitamin B1 in human blood serum samples.

In 2015, Tan and co-workers (Tan et al., 2015) demonstrated the peroxidase-like activity of copper-based MOFs (HKUST-1) by employing vitamin B1 as a peroxidase substrate. In the presence of H_2O_2, HKUST-1 can catalyze efficiently the conversion of non-fluorescent vitamin B1 to strong fluorescent thiochrome. HKUST-1 has the features of Michaelis–Menten behaviors and shows stronger affinity to vitamin B1 than horseradish peroxidase (HRP). Based on the peroxidase-like activity of HKUST-1, a simple and sensitive fluorescent method for vitamin B1 detection has been developed. As low as 1 mM vitamin B1 can be detected with a linear range from 4 to 700 mM. The detection limit for vitamin B1 is about 50-fold lower than that of HRP-based fluorescent assay. The proposed method was successfully applied to detect vitamin B1 in tablets and urine samples.

In 2013, Kamruzzaman and co-workers (Kamruzzaman, et al., 2013) were analyze vitamin B1 by chemiluminescence (CL) method on a microchip. The microchip was fabricated by soft lithographic procedure using polydimethyl siloxane (PDMS). The method is based on the enhanced CL intensity of luminol by its oxidation with $AgNO_3$ in the presence of platinum nanoparticles (PtNPs). It was found that the CL intensity of the luminol–$AgNO_3$–PtNPs system was further increased with the addition of vitamin B1. Under optimum conditions, the linearity range of vitamin B1 concentration is 1.0×10^{-7} to 4.0×10^{-5} $molL^{-1}$ with a correlation coefficient of 0.9992. The limit of detection was found to be 4.8×10^{-9} $molL^{-1}$. The method was successfully applied to determine vitamin B1 in vitamin tablets.

In 2013, Zhan and co-workers (Zhou et al., 2013) were investigated electrochemical sensing based on green emissive gold nanoparticles and nanorods

(AuNR-TbM-EDTA/GCE) for determination of vitamin B1 in water. A luminescent terbium complex was covalently modified onto anisotropic gold nanostructures (nanopar-ticles and nanorods) respectively. AuNR-TbM-EDTA/GCE were fabricated by anchoring gold nano-sensors on the surface of glassy carbon electrodes. Both the fluorescence spectra and cyclic voltammetry curves exhibited selective signal changes in the presence of vitamin B1 in comparison with vitamin B2, B3, B4, B5 and B6. The detection limit of this probe for vitamin B1 is 6.3×10^{-7}M. It is considered to be the first example that different dimensional fluorescent nano-probes were selected and applied as dual opto-electrochemical sensors for recognizing the same analyte.

In 2007, Wang and co-workers (Wang, Liu, Kong, & Liu, 2007) were report the developed method for the determination of Vitamin B1 with nanoparticles as a probe by resonance Rayleigh Scattering (RRS) technique. In the presence of I^- excess, copper nanoparticles (Cu_n) were prepared by using the reduction reaction of $NaBH_4$ and copper sulphate. In the solution, I anions self-assemble on the surface of Cu nanoparticles which become large anionic complexes $[Cu_nI_m]$. Resulting in the change of the absorption spectrum and great enhancement of RRS intensity. The maximum scattering wavelength is 369 nm. There was a linear relationship between the RRS intensity (ΔI) and the Vitamin B1 concentration in the range of 0.02–0.40 mg l^{-1}. The detection limit for vitamin B1 was 6.4 μg l^{-1}.

7.2 Literature review for the determination of calcium

In 2017, Yu and co-workers (Yu et al., 2017) developed a novel flowing liquid cathode glow discharge (LCGD) as an excitation source of the atomic emission spectrometry (AES) for the determination of Ca and Zn in digested calcium and blood samples, in which the glow discharge is produced between the electrolyte over flowing from a quartz capillary and the needle-like Pt anode. The electron temperature and electron density of LCGD were calculated at different discharge voltages. The results showed that the optimized analytical conditions are pH = 1 HNO_3 as supporting electrolyte, 4.5 mL min^{-1} solution flow rate. The power consumption of LCGD is 43.5–66.0 W. The limits of detections (LODs) for calcium are 0.011–0.097 mg L^{-1}, which are in

good agreement with the closed-type electrolyte cathode atmospheric glow discharge (ELCAD). The obtained results of calcium in real samples by LCGD-AES are basically consistent with the ICP-AES and reference value. The results suggested that LCGD-AES can provide an alternative analytical method for the detection of metal elements in biological and medical samples.

In 2017, Maryam and co-workers (Maryam, Hajinia, & Heidari, 2017) presented a novel and low-cost method for the fabrication of microfluidic paper using sticker templates with specific patterns and a waterproof eye pencil. The proposed fabrication process could be finished within 10 minutes without using complicated instruments. To verify the applicability of the fabricated microfluidic paper, colorimetric assays were performed for simultaneous analysis of calcium and magnesium by single and multiple indicators. The limit of detection is 8.3 mg L^{-1} and 1.0 mg L^{-1}, and the relative standard deviation is 8.3% and 5.9% for calcium and magnesium, respectively. In the paper based microfluidic device, a linear range from 10 to 100 mg L^{-1} for calcium. The concentration of calcium and magnesium were successfully determined in tap, river, mineral, and household purifier water samples.

In 2016, Karita and Kaneta (Karita & Kaneta, 2016) developed microfluidic paper-based analytical devices for the chelate titrations of calcium and Mg^{+2} in natural water. The microfluidic paper-based analytical devices consisted of ten reaction zones and ten detection zones connected through narrow channels to a sample zone located at the center. Buffer solutions with pH of 10 or 13 were applied to all surfaces of the channels. A metal indicator (Eriochrome Black T or Calcon) was added to the detection zones and different amounts of ethylenediaminetetraacetic acid (EDTA) were added to the reaction zones. The total concentrations of calcium and magnesium (total hardness) in the water were measured using a microfluidic paper-based analytical device containing a buffer solution with a pH of 10, whereas only calcium ion was titrated using a microfluidic paper-based analytical device prepared with a potassium hydroxide solution with a pH of 13. The microfluidic paper-based analytical devices were

successfully determined of calcium and Mg^{+2} in mineral, river and sea water samples within a few minutes using only the naked eyed no need of instruments.

In 2013, Lopez-Molinero and co-workers (Lopez-Molinero, Cubero, Irigoyen, & Piazuelo, 2013) displayed the application of basic RGB colors in Digital Image-Based Colorimetry for water calcium hardness determination. The proposed method was carried out using the chromogenic model formed by the reaction between calcium and glyoxal bis(2-hydroxyanil). It produced orange–red colored solutions in alkaline media. To evaluation evidenced that the highest variance of the system and the highest analytical sensitivity were associated to green color. However, after the study by Fourier transform the basic red color was recognized as an important feature in the information. RGB intensities were linearly correlated with calcium in the range 0.2–2.0 mgL^{-1}. In the optimum conditions, using green color, a simple and reliable method for Calcium determination could be developed. The detection limit was 0.07 mgL^{-1}. Water of the city, mineral bottled, and natural-river were analyzed. The results were compared and evaluated with a flame atomic absorption spectroscopy and titrimetric method. The potentiality of the procedure as a field and ready-to-use method was probed.

From previous research, there conventional methods to detect vitamin B1 or calcium with highly selective, sensitive and accurate quantification but these methods are expensive, complicated and time-consuming. Hence, the colorimetric assay base on gold nanoparticles have attracted increasing attention as a result of their simplicity, no need complex instruments, inexpensive, outstandingly prompt measurement and adequate miniaturization of the sensing devices with high sensitivity and selectivity.

CHAPTER III
METHODOLOGY

This chapter describes the chemicals and instruments, the chemical preparation, experiments procedure and detection method used in this work. The experimental section is presenting research methodology which is dividing to 2 parts: (1) developing a colorimetric method using gold nanoparticles for the detection of vitamin B1 in urine (2) developing a colorimetric method using 4-Amino-6-hydroxy-2-mercaptopyrimidine monohydrate (AHMP) modified gold nanoparticles for the detection of calcium in urine.

1. Materials

Materials used in this study can be grouped as described in Table 3.

1.1 Chemicals

All chemicals used in this study were analytical reagent (AR) grade and solutions were prepared using high pure water with a resistance of 18 MΩcm^{-1}.

Table 3 Chemicals used in this research.

Order	Reagents	Suppliers
1	AuNPs solution Diameter 20 nm, 0.01%W/V	Kestrel Bio Sciences, Thailand
2.	Thiamine hydrochloride (vitamin B1)	Ajax Finechem Pty Ltd., AUS

Table 3 (Continued)

Order	Reagents	Suppliers
3.	4-Amino-6-hydroxy-2-mercaptopyrimidine monohydrate(AHMP)	Sigma-Aldrich, USA
4.	Calcium chloride ($CaCl_2$)	Ajax Finechem Pty Ltd., AUS
5.	Riboflavin (vitamin B_2), D-pantothenic acid (vitamin B_5), Folic acid (vitamin B_9), Vitamin B_{12}, Uric acid, Glucose, and Ascorbic acid (Vitamin C)	Sigma-Aldrich, USA
6.	Niacin (vitamin B_3) and pyridoxine hydrochloride (vitamin B_6)	Himedia Laboratories Pvt Ltd., India
7.	Disodium Phosphate (Na_2HPO_4)	Ajax Finechem Pty Ltd., AUS
8.	Monosodium Phosphate (NaH_2PO_4)	Ajax Finechem Pty Ltd., AUS
9.	Sodium Hydroxide (NaOH)	Ajax Finechem Pty Ltd., AUS
11.	Copper sulphate, ($CuSO_4$), barium chloride ($BaCl_2$), cadmium chloride ($CdCl_2$), mercurry chloride ($HgCl_2$), and zinc sulphate ($ZnSO_4$)	Ajax Finechem Pty Ltd., AUS
12.	Potassium hexacyanoferrate(III)	Sigma-Aldrich, USA
13.	Artificial urine	Carolina biological company, USA

1.2 Instrumentation

- Wax printer (Xerox 8570, Fuji, Japan)

- Transparency sheets

- A digital camera (Power Shot S95, 10.1 Megapixels, Canon)

- pH meter (Metrohm, Mettler Toledo)

- Balance 4 positions (AG204, Mettler Toledo)

- UV–visible spectrometer (UV-2450 UV-visible spectrophotometer, SHIMADZU)

- Fluorescent (FP-8300, Jasco Spectrofluorometer)

- An atomic absorption spectrometer (AAS) with a hollow cathode lamp and standard air/acetylene flame (Analyst 300, Perkin Elmer Instruments, USA). A hollow cathode lamp for the determination of calcium was used under the following operations conditions: wavelength: 324.8 nm; slit- width: 0.70 nm; lamp current: 25 mA

1.3 Preparation

1.3.1 Preparation of pre-concentration of gold nanoparticles

Pre-concentration of gold nanoparticles was prepared by pipetting 1 ml of the commercial gold nanoparticles into a micro centrifuge tube. After that, 20 micro centrifuge tubes from the first step was centrifuged at 12,000 rpm (4°C) for 30 min. Then the 0.8 mL of supernatant (clear) solution was removed and the 0.2 mL of remaining (dark red) solution was stirred for 10 seconds. Repeat the same process for stock the pre-concentrated gold nanoparticles.

AuNPs size 20 nm 0.01%w/v   12,000 rpm 4°C 30 min

Concentrated AuNPs   Stir for 10 seconds
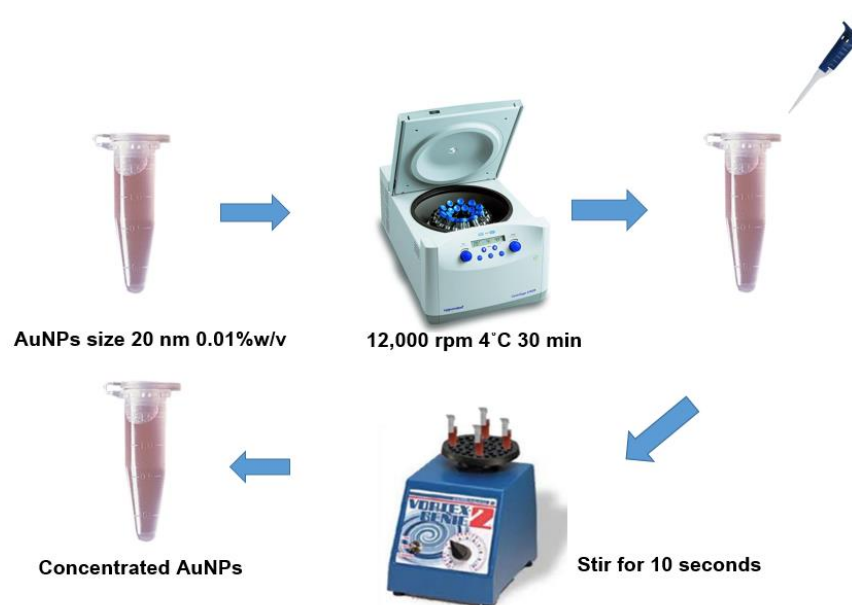
Figure 11 Schematic diagram for the pre-concentration of gold nanoparticles procedure.

1.3.2 Preparation of AHMP-modified gold nanoparticles (AHMP-AuNPs)

AHMP-AuNPs was prepared by mixing 0.10 mL of 4 mM AHMP into 1.50 mL of the pre-concentration AuNPs solution. After that, the mixture solution was stirred for 15 minutes to ensure a complete self-assembly of AHMP onto the surface of AuNPs. AHMP-AuNPs was fresh preparation before use.
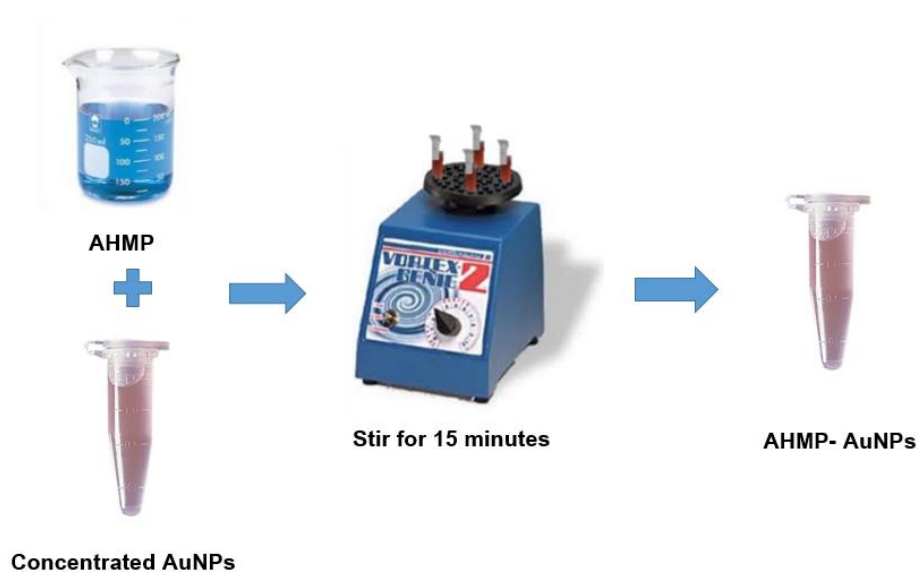
Figure 12 Schematic diagram for the AHMP-modified gold nanoparticles (AHMP-AuNPs) procedure.

1.3. 3 Fabrication transparency sheet-based devices

A portable vitamin B1 and calcium detection device was fabricated on a transparency sheet using wax printing method. Which the pattern was designed by using Microsoft Power Point. The fabrication process has only two steps. First, the wax pattern was printed on the transparency sheet using the wax printer (Xerox 8570, Fuji, Japan). A transparency sheet-based devices was designed to the circle shape with detection zone is 5 mm. diameter. The maximum of liquid can hold in the detection zone is 30 μL. The wax covered area was hydrophobic, while the area without wax was hydrophilic as detection area. Second, the tape was attached the back side of the transparency sheet to white paper (paper A4, 500 grams). Using this process, the transparency sheet-based devices can be fabricated within 2 minutes.

Pattern design   Wax printing   Transparency based analytical devices

Figure 13 Fabrication process of pattern paper by wax printing.

1.3.4 Preparation of phosphate buffer pH 6.0

The solution A was prepared by weighting Na_2HPO_4 1.4200 g. The solution B was prepared by weighting NaH_2PO_4 1.5600 g. Each salt was dissolved in 100 mL of 18 $M\Omega cm^{-1}$ water. The solution A and B were pipetted the volume of 0.308 mL and 2.193 mL, respectively and were mixed together. Then, the mixture was adjusted the volume to 50.00 mL.

1.3.5 Preparation of phosphate buffer pH 7.0

The solution A was prepared by weighting Na_2HPO_4 1.4200 g. The solution B was prepared by weighting NaH_2PO_4 1.5600 g. Each salt was dissolved in 100 mL of 18 $M\Omega cm^{-1}$ water. The solution A and B were pipetted the volume of 1.525 mL and 0.975 mL, respectively and were mixed together. Then, the mixture was adjusted the volume to 50.00 mL.

1.3.6 Stock solution of 500 ppb vitamin B1

Vitamin B1 was weighed 0.0025 g and dissolved in 500.00 mL of phosphate buffer pH 7.0. The stock solution of 500 ppm vitamin B1 was diluted to the concentration of 5, 10, 20, 30, 40, 50, 60, 70, 80, 90, 100, 200, 300 and 400 ppm by phosphate buffer pH 7.0.

1.3.7 Stock solution of 500 ppm calcium

$CaCl_2$ was weighed 0.0100 g and dissolved in 50.00 mL of phosphate buffer pH 6.0. The stock solution of 500 ppm calcium was diluted to the concentration of 5, 10, 20, 30, 40, 50, 60, 70, 80, 90, 100, 200, 300 and 400 ppm by phosphate buffer pH 6.0.

2. Experimental

Part 1: Developing a colorimetric method using gold nanoparticles for the detection of vitamin B1 in urine

2.1 Optimum conditions

In this section, various optimization parameters including AuNPs concentration, AuNPs and vitamin B1 volume ratio, pH and the incubation time were examined. The colorimetric detection of vitamin B1 was performed at room temperature by drop sequentially of AuNPs and vitamin B1 on the detection zone of transparency sheet-based devices. The Δ red intensity was measured by using camera for captured the picture and image J software for calculated the red color intensity with computer. The resulting of aggregation capability between vitamin B1 and AuNPs in each condition was observed using Δ red intensity form transparency sheet image. The concentration of gold nanoparticles was varied in the range of 100, 125, 167, 250 and 500 ppm. The aggregation of AuNPs induced by vitamin B1 was investigated at various incubation times (2 – 30 min). After that, the effect of AuNPs and vitamin B1 volume ratio as well as pH effect were studied in the range of 1:5 to 5:1 and pH 2-10, respectively.

2.2 Colorimetric measurement of vitamin B1 using AuNPs probe

After getting the optimum condition for the colorimetric measurement of vitamin B1 using AuNPs probe, a determination of vitamin B1 was made. Various concentration of vitamin B1 were prepared by using serial dilution of stock solution by 0.01 M phosphate buffer pH 7 (NaH_2PO_4 and Na_2HPO_4) to determine the linearity and sensitivity of AuNPs. Colorimetric detection of vitamin B1 were performed at room temperature by dropping 15 μL of concentrated AuNPs and 15 μL of different concentrations of vitamin B1 on detection zone of the transparency sheets and the AuNPs aggregation was monitored thereafter. The AuNPs aggregation with vitamin B1 on the transparency sheets were captured using digital camera and then analyzed using Image J software. The limit of detection (LOD) and the limit of quantitation (LOQ) were calculated as 3 SD_{bl}/S and 10 SD_{bl}/S, respectively, where SD_{bl} is the standard deviation of the blank

measurement (n=10) and S is the sensitivity of the method obtained as the slope of the calibration curve.

2.3 Method validation experiments

The application of the present method was evaluated with fluorescent method by determining vitamin B1 in urine samples. Fluorescent method is one of the most important methods which used to measure the level of vitamin B1 present in a sample. vitamin B1 or thiamin was to change it to the florescent thiochrome derivative; this method was first reported by Jansen in 1936 (Jansen, 1936). Thiochrome is produced by the oxidation of vitamin B1 in an alkaline medium with potassium hexacyanoferrate(III).

This experiment employs fluorescence intensity to quantify thiamine (vitamin B1) which is oxidized to fluorescent thiochrome. The following three solutions are prepared.

1. Potassium hexacyanoferrate(III) (K_3FeCN_6) 0.001g was dissolved in DI water, and then diluted to 100 ml to make a 10 ppm K_3FeCN_6 solution.

2. Thiamine hydrochloride stock solution: (10,000 ppb): a 0.0005 g amount of pure thiamine HCl was dissolved in DI water and complete to 50.00 ml volumetric flask. A standard vitamin B1 stock solution was prepared and stored in the dark. Then prepare five working standards, vitamin B1 working solution (300, 200, 150, 100, and 50 ppb) was prepared by diluted (0.3, 0.2, 0.15, 0.1, and 0.05 ml) of the stock solution to 10.00 ml volumetric flask with DI water.

3. The buffer pH = 12.2 is prepared from reagent grade NaH_2PO_4 (0.2900 g) and Na_2HPO_4 (3.2300 g) in 100 mL of water to make a 0.2 M buffer. Sodium hydroxide or phosphoric acid is added to bring the pH to 12.2.

2.3.1 Analytical procedure for calibration

Add 1.00 mL of the 0.2 M phosphate buffer (pH = 12.2) into the (fluorescence) sample cuvette. Then add 1.00 mL of the 10 ppm K_3FeCN_6 solution into the cuvette. After that add 1.00 mL of the standard to be analyzed. Cap the cuvette quickly and invert a few times to ensure adequate mixing and then place in the spectrofluorometer. Close the sample compartment. The fluorescence intensity generated by thiochrome produced immediately at λ_{ex} = 369 nm and λ_{em} = 436 nm. Repeat the above steps for all the working standards.

Part 2: Developing a colorimetric method using 4-Amino-6-hydroxy-2 mercaptopyrimidine monohydrate (AHMP) modified gold nanoparticles for the detection of calcium in urine

2.4 Optimum conditions

In this section, various optimization parameters including the modifier volume ratio, pH, the incubation time and AHMP-AuNPs: samples volume ratio were examined. The colorimetric detection of calcium was performed at room temperature by drop sequentially of AHMP-AuNPs and calcium on the detection zone of transparency sheets. The red/blue intensity was measured by using camera for captured the picture and image J software for calculated red and blue color intensity with computer. The resulting of aggregation capability between calcium and AHMP-AuNPs in each condition was observed using the red/blue intensity form transparency sheet image. First, the volume of 4 mM AHMP modifier was varied in the range of 0.1, 0.2, 0.4, 0.6, 0.8, 1.0, 1.2 and 1.5 mL at the same pre-concentered AuNPs volume (1.5 µL). Then, 15 µL of the varied AHMP-AuNPs were investigated with 15 µL of calcium at 0, 10, 50 and 100 ppm concentration, respectively. The aggregation of AuNPs induced by calcium was investigated at various incubation times (2 – 30 min). After that, the effect of AuNPs and calcium volume ratio and pH effects were studied in the range of 1:5 to 5:1 and pH 2-10, respectively.

2.5 Colorimetric detection of calcium

The calcium standard solution was made by appropriate dilution of the stock solution on a daily basis as required. A colorimetric analysis of calcium was performed as follows. First, 5 µL of calcium solution or samples (pH 6.0 PBS) were added into detection zone of transparency sheet-based device follow by addition of 25 µL of AHMP-AuNPs. Then the red/blue intensity of AHMP-AuNPs mixed with calcium standard solution was captured by camera and measured via image J software, respectively. Under the optimal conditions, the relationship between the red/blue intensity of triplicate measurements and concentrations of calcium solution between 10 – 100 ppm was plotted to observe linear range.

2.6 Validation for calcium analysis

Under the optimal conditions, the proposed method was applied for the determination of calcium in artificial urine samples by standard addition method. The artificial urine was purchased from Carolina biological supply company. The proposed method was validated against atomic absorption spectrophotometry (AAS). 0.0347 g. of $CaCl_2$ was added to 25 mL of artificial urine for preparation the 500 ppm calcium stock solution. Then the stock solution was diluted with artificial urine to 320, 160, and 80 ppm of calcium concentration. The samples were adjusted to pH 6 by the addition of 3 M sodium hydroxide and the urine added to reach a final volume. Prior analysis with the proposed method 320 and 160 ppm of calcium concentration samples were diluted with 50 mM phosphate buffer pH 6 for 4-fold and 2-fold, respectively. For AAS method, the samples 320, 160, and 80 ppm of calcium concentration were diluted with 50 mM phosphate buffer pH 6 for 150-fold, 45-fold, and 80-fold, respectively. (AAS can detect within range 0.5-5 ppm)

3. Image J measurement

The results were recorded by camera. After that, it will be used to determine intensity with Image J program. The Image was clicked on the toolbar, and then selects

the button, and select type was RGB stack. The statement threshold color to red, green and blue, respectively. The average intensity of (red or blue) colors were determined by pressing the analyze button on the toolbar, and then select measure.

CHAPTER IV

RESULTS AND DISCUSSION

Colorimetric method using gold nanoparticles were sequentially developed to analysis of vitamin B1 and calcium in urine samples with a simple transparence sheet-based device. Initial experiments and fabrication of the device were described in Chapter 3. This chapter aims to present the findings and discussion of this study.

1. Development of colorimetric method using gold nanoparticles for an analysis of vitamin B1 by transparence sheet-based devices

1.1 Optimization conditions for gold nanoparticles colorimetric sensing for vitamin B1 by transparence sheet-based devices

1.1.1 Optimization of AuNPs concentration

First, pre-concentration of gold nanoparticles was prepared for vary AuNPs concentration at 100, 125, 167, 250, and 500 ppm as shown in Figure 14 (a) and the red intensity at vary concentration of AuNPs were shown in Figure 14 (b). To demonstrate valuable change of color between AuNPs and vitamin B1 300 ppb (exceed concentration for check limit of the aggregation), the AuNPs concentration at 100, 125, 167, 250, and 500 ppm were optimized. The red intensity was calculated from picture by using image J software mode RGB stack and measure the Δ red intensity for the aggregation between AuNPs and vitamin B1 to change has been monitored simultaneously as shown in Figure 15. The Δ red intensity was increased with increasing concentration of AuNPs as shown in Figure 15 (d), so the concentration of AuNPs at 500 ppm is an appropriate concentration.

a)

b)
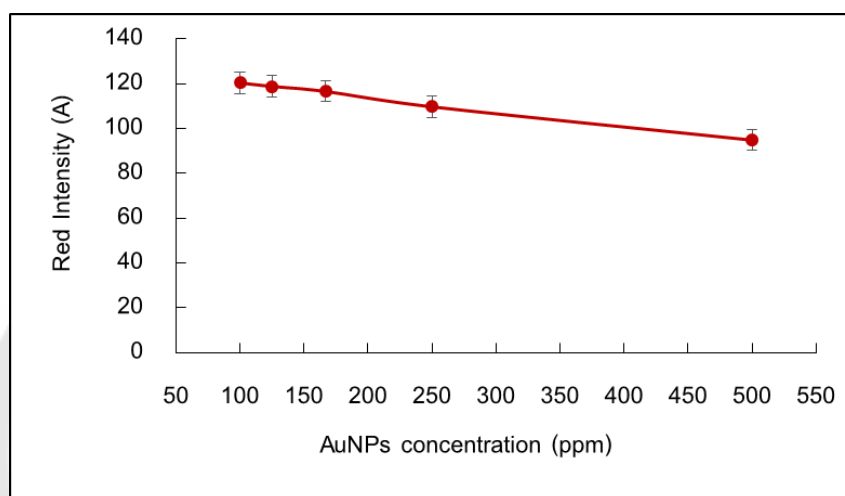
Figure 14 a) The color of AuNPs concentration at 100, 125, 167, 250, and 500 ppm after per-concentration process and b) Linear correlation of red intensity as a function of AuNPs concentration.
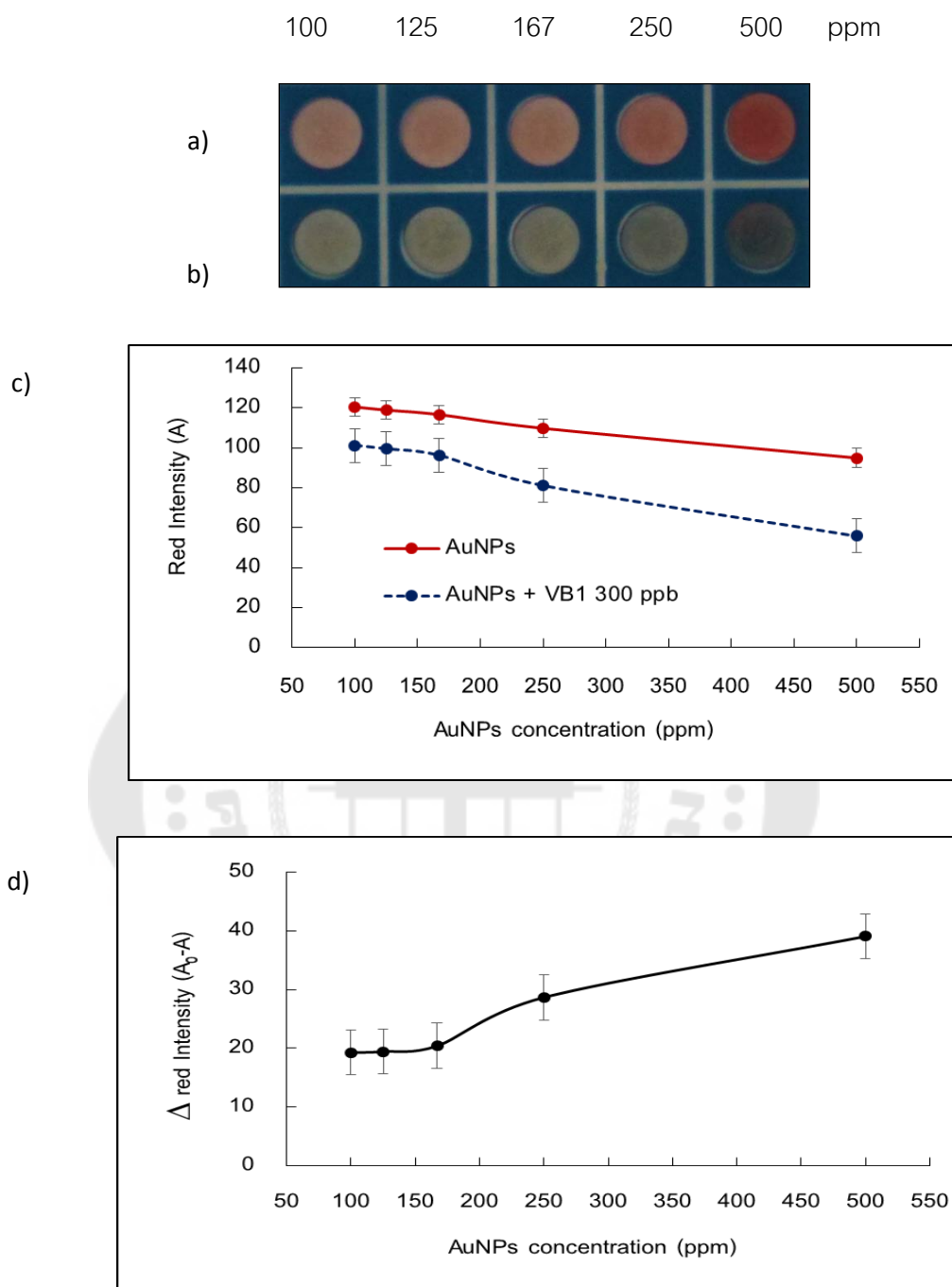
Figure 15 The color changes of the aggregation between: a) AuNPs mixed with buffer b) AuNPs concentration at 100, 125, 167, 250, and 500 ppm, respectively mixed with vitamin B1 at 300 ppb c) Linear correlation of red intensity as a function of AuNPs concentration and d) Linear correlation of the Δ red intensity as a function of AuNPs concentration.

1.1.2. Optimization of AuNPs and vitamin B1 volume ratio

The detection zone of the transparency sheets had miximum volume of 30 µL. The color change of the aggregation between AuNPs and vitamin B1 100 ppb volume ratio at 1:5, 1:2, 1:1, 2:1 and 5:1 were shown in Figure 16 and the color change of the aggregation between AuNPs and vitamin B1 300 ppb volume ratio at 1:5, 1:2, 1:1, 2:1 and 5:1 were shown in Figure 17. The Δ red intensity was maxiumum at 1:1 volume ratio. Then, 15 µL of AuNPs:15 µL of vitamin B1 was chosen for further experiments to provide the preferable sensitivity for vitamin B1 detection.
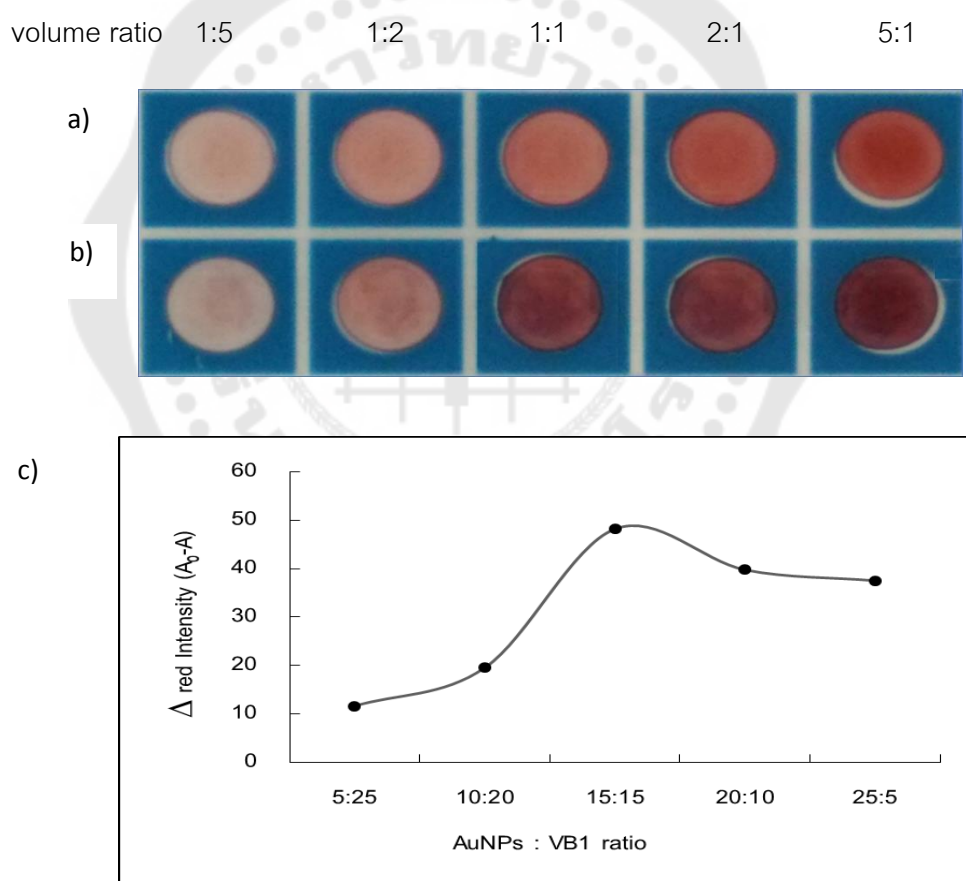
Figure 16 The color changes of the aggregation between: a) AuNPs mixed with buffer b) AuNPS mixed with vitamin B1 100 ppb at volume ratio 1:5, 1:2, 1:1, 2:1 and 5:1, respectively and c) Linear correlation of the Δ red intensity as a function of AuNPs: 100 ppb vitamin B1 ratio.

volume ratio   1:5   1:2   1:1   2:1   5:1
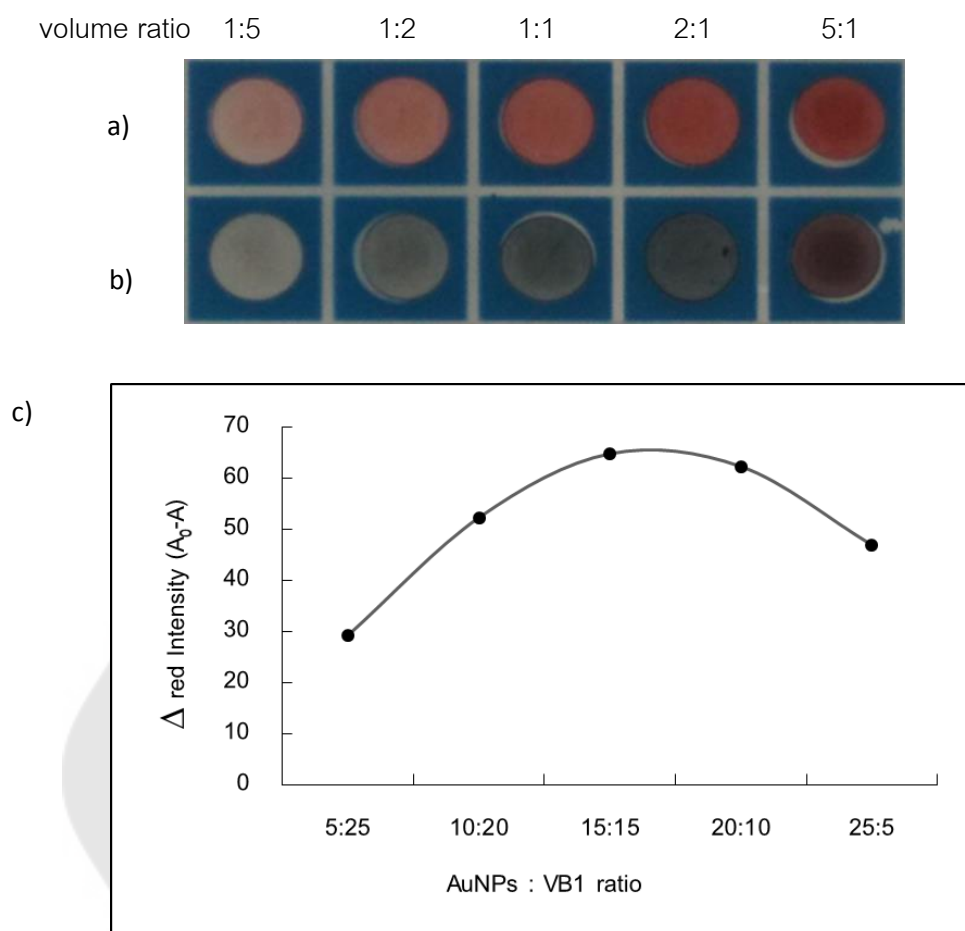
Figure 17 The color changes of the aggregation between: a) AuNPs mixed with buffer b) AuNPS mixed with vitamin B1 300 ppb at volume ratio 1:5, 1:2, 1:1, 2:1 and 5:1, respectively and c) Linear correlation of the Δ red intensity as a function of AuNPs: 300 ppb vitamin B1 ratio.

1.1.3 Optimization of pH buffer

The effects of the pH buffer on the aggregation between the AuNPs and vitamin B1 were examined by varying the pH of the buffer from 2 to 10. In principle, vitamin B1 is positively charged on both the pyrimidine N1 nitrogen ($pK_{a1} \cong 4.8$) and thiazole N3 nitrogen at low pH, and vitamin B1 exists as a cation with a positive charge on the thiazole N3 nitrogen at physiological pH. As the pH further increases, vitamin B1

exists as an uncharged pseudo base intermediate, which displays a negatively charged thiol form ($pK_{a2} \cong 9.2$). As a result, the similarly charged AuNPs and vitamin B1 repelled each other when the pH was higher than 7. Therefore, pH 7.0 was chosen for the experimental buffer in the following study. In addition, it was found that when using a pH 7 buffer, the Δred intensity of the related vitamin B samples changed slightly, while the Δred intensity of vitamin B1 was obviously changed, as shown in Figure 18. From this finding, a 10 mM phosphate buffer at pH 7 was suitable for the sensitive and selective detection of vitamin B1 by this colorimetric method.
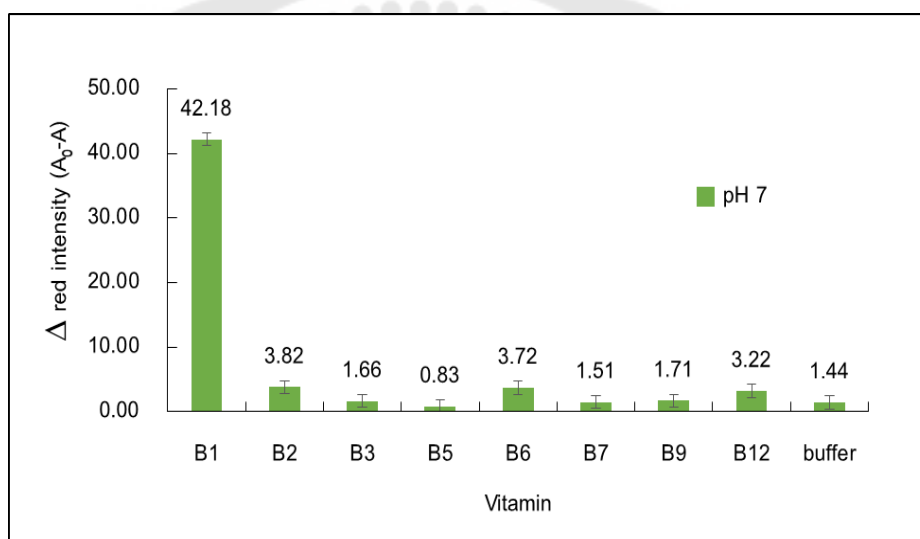
Figure 18 Effects of 10 mM phosphate buffer pH 7 on the aggregation between AuNPs and 100 ppb of vitamin B1.

1.1.4 Optimization of incubation time

The incubation time in the range of 2 to 30 minutes were optimized. The Δ red intensity was calculated from the color change of picture which was captured and measured intensity by image J sofeware. The Δ red intensity was shown in figure 19. The Δ red intensity was increased with increasing incubation time and maxiumum at 10 minutes. The Δ red intensity was decrease after 10 minutes because the precipitation

may be occur. From the results, the optimal incubation time is 10 minutes. These conditions are provided the highest different color change intensity.
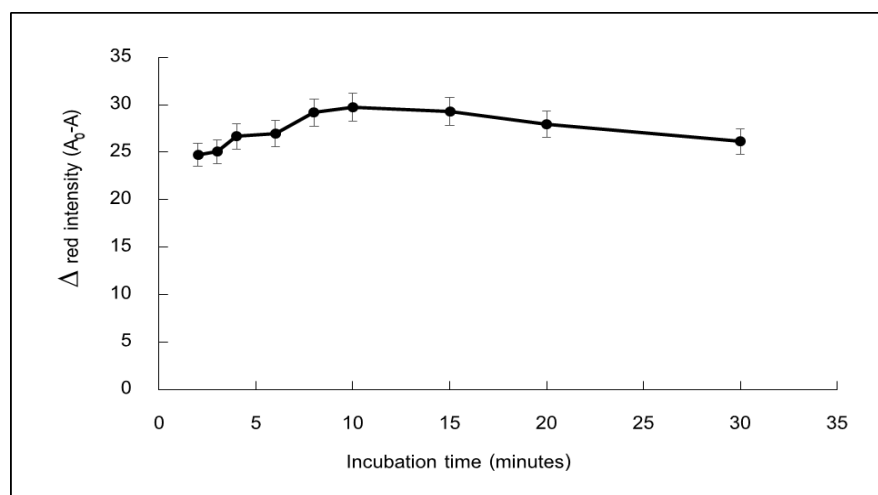
Figure 19 The effects of incubation time on the detection of vitamin B1 concentration at 100 ppb.

1.2 Calibration curve

The study of calibration curve was obtained from Δ red intensity which measured by camera. First, 15 µL of concentrated AuNPs was dropped on transparence sheet then was added 15 µL of standard (vitamin B1) solution for 10 minutes incubation time. For the increase of vitamin B1 concentration, the Δ red intensity of AuNPs was decrease because AuNPs color changed from red to blue and corresponds to results from UV-vis spectrophotometer in Figure 21. In Figure 20, a linear relationship between the Δ red intensity and vitamin B1 concentration was established. The Δ red intensity of AuNPs is directly proportional to the added vitamin B1 concentration. A good linearity was observed in the concentration range of 40 to 200 ppb of vitamin B1 with a correlation coefficient of 0.9913. The limit of detection (LOD) and limit of quantitation for vitamin B1 were found to be 3.00 ppb and 10.01 ppb (N=3), respectively. (LOD = 3 x $10^{(0.0241/92.023)}$), SD_{bl} = 0.0241 is the standard deviation of the

blank measurement (n=10) and S = 92.023 is the sensitivity of the method obtained as the slope of the calibration curve.
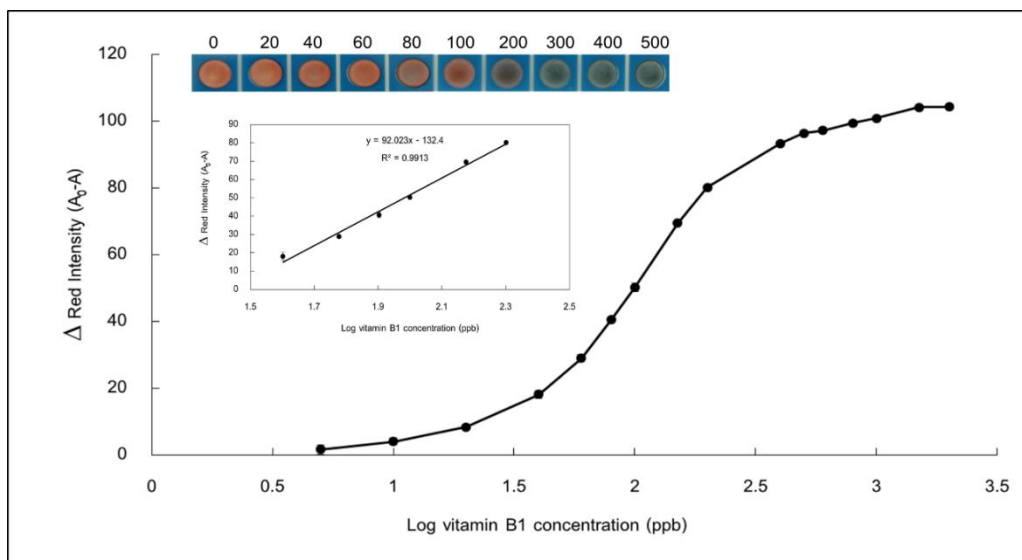
Figure 20 Calibration curve plot of different red intensity versus varied vitamin B1 concentrations.
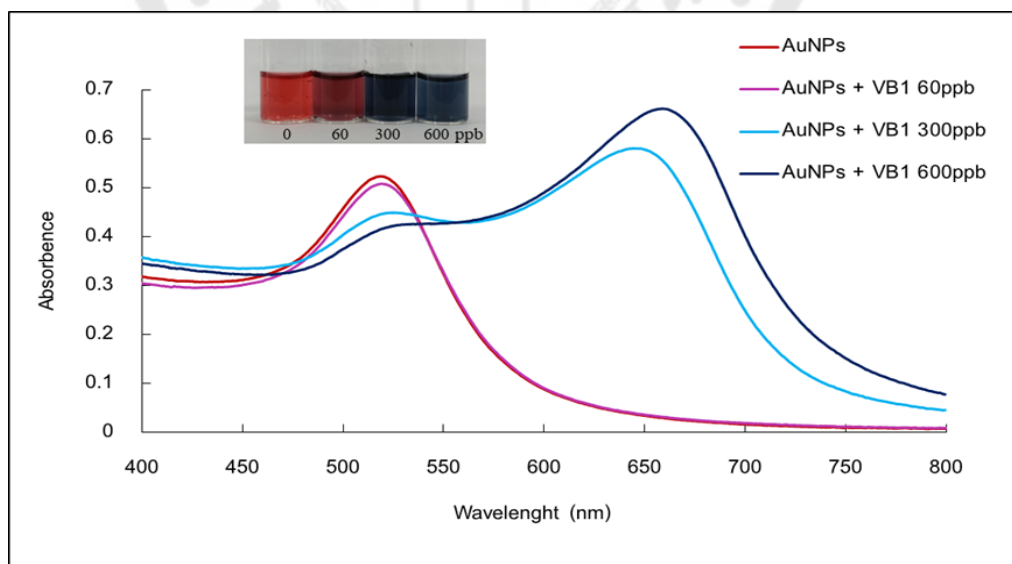
Figure 21 UV-vis absorption spectra and photographs of the AuNPs after the addition of vitamin B1 at different concentrations, measured 10 minutes after addition.

1.3 Selectivity of AuNPs for vitamin B1 detection

To investigate selectivity of AuNPs for vitamin B1 detection, relevant vitamin B complexes including vitamin B2, vitamin B3, vitamin B5, vitamin B6, vitamin B7, vitamin B9, vitamin B12 and vitamin C were also tested. The color signal change in the AuNPs in the presence of other vitamin species and common interfering molecules had a less than ± 5% change compared to that of the color signal of only vitamin B1 (20 ppb). As shown in Figure 22, the other vitamin species and common interfering molecules have no appreciable change. The achieved high experimental selectivity and sensitivity is due to the strong electrostatic interactions between the positively charged vitamin B1 and negatively charged AuNPs.
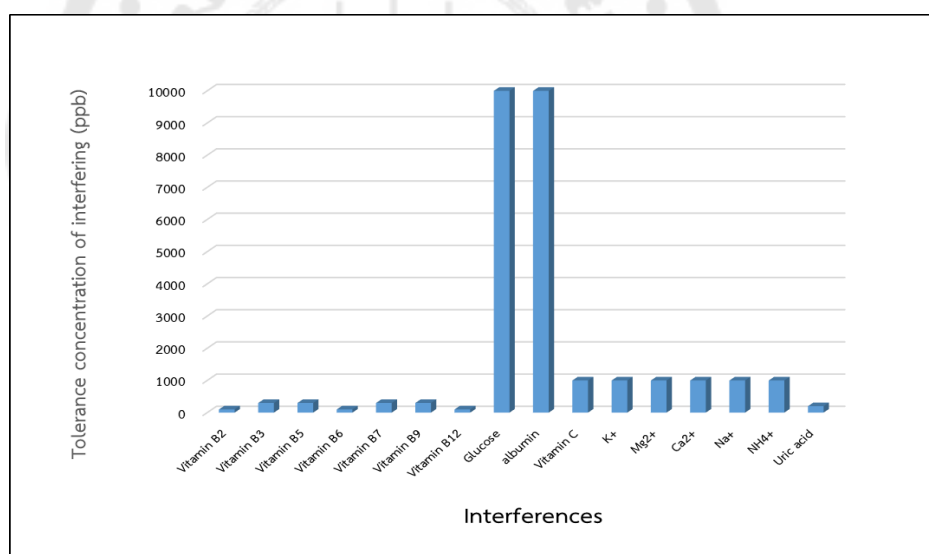
Figure 22 The tolerance concentration of other vitamin species and common interfering molecules.

1.4 Analytical application in a real sample

To evaluate the efficiency of our method, the colorimetric sensor was used to detect vitamin B1 in urine samples. Under the optimal conditions, the determination of vitamin B1 in urine samples spiked with vitamin B1 is shown in Table 4. The recoveries

and %RSDs for vitamin B1 were in the range of 84.72 - 91.08 % and 2.74 – 6.98 %, respectively. Moreover, the results for the vitamin B1 values obtained by the developed sensor were compared with the reference values obtained using a standard method, as shown in Table 4. As a result, this proposed colorimetric sensor can be applied for the determination of vitamin B1 in the urine samples with satisfactory results.

Table 4 The %RSD and %Recovery for determination of vitamin B1 in urine samples (n=10).

| vitamin B1 spiked (ppb)	vitamin B1 (ppb)		% RSD (n=10)	% Recovery
	This Method	Fluorometric method		
40	36.43 ± 1.00	41.53 ± 0.63	0.61	91.06
60	50.83 ± 3.55	63.55 ± 0.68	2.26	84.72
80	69.06 ± 3.40	79.02 ± 0.50	2.29	86.32

2. Development of colorimetric method using gold nanoparticles for an analysis of calcium by transparence sheet-based devices

2.1 Modification and characterization of AHMP-AuNPs

To investigate the incorporation of AHMP onto the AuNPs surface. UV-vis spectroscopy and Zeta potentials were respectively performed. Figure 23 shows the UV-vis spectra of AHMP, AuNPs and AHMP-AuNPs. The localized surface plasmon resonance (LSPR) absorption peak of AHMP has the maximum peak at 275 nm. While, the AuNPs has only the maximum peak at 519 nm. After the AuNPs were modified with AHMP, the UV-vis spectra of AHMP-AuNPs show significantly the maximum peak at 273 and 523 nm. We believe that the added peak and the red-shifted band are mainly caused by the decrease of the plasma oscillation frequency around the nanoparticles from the binding between thiol-containing compounds and the gold nanoparticles. Corresponding with the zeta potential results, the surface charge of AuNPs and AHMP-

AuNPs were displayed the negative charge at -43.1 and -49.9 mV, respectively. The zeta potentials were indicated the negative charge of AuNPs increasing from -43.1 mV (intensity 32 a.u.) to -49.9 mV (intensity 38 a.u.) as shown in Table 5. The surface of AHMP-AuNPs have more negative charge. It is expected that the thiol group of AHMP is chemisorbed on the surface of AuNPs whereas amine and hydroxyl groups available in AHMP are free from binding. The presence of lone pair electrons of amine groups and hydroxyl groups were indicated the negative charge around the AuNPs surface (S. Shankar & S.A. John, 2015). This result displayed that AHMP had been completed modified onto the surface of AuNPs.
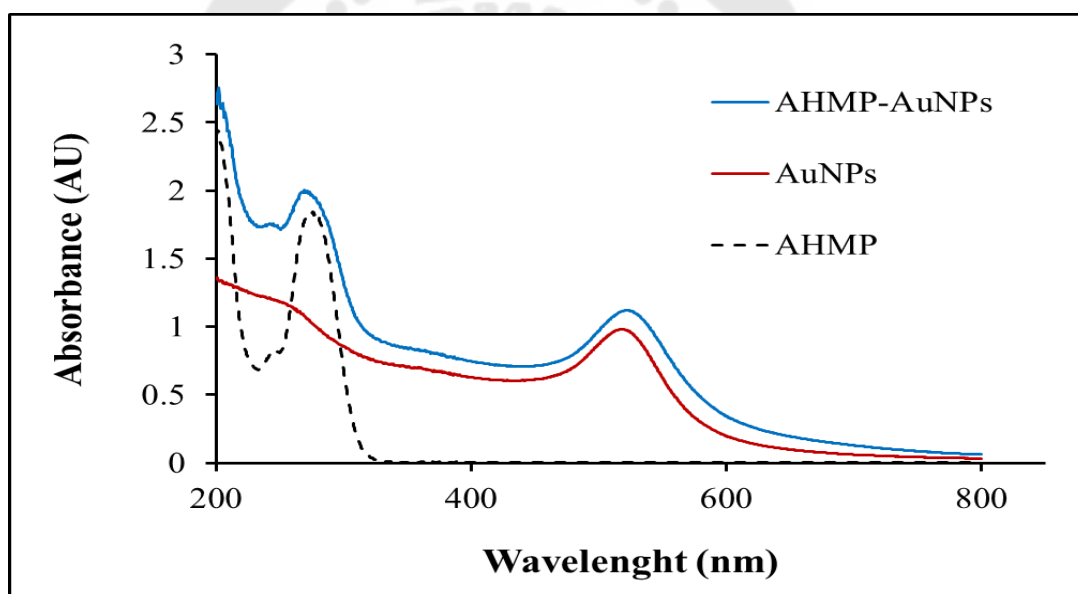
Figure 23 UV- vis absorption spectra of AHMP, AuNPs and AHMP-AuNPs.

Table 5 Zeta potential measurement of AHMP, AHMP-AuNPs, Buffer-AHMP-AuNPs and calcium -Buffer-AHMP-AuNPs

Samples name	Z-Average (nm)	Zeta Potential (mV)	Intensity (a.u.)
AuNPs	26.9	-43.1	32
AHMP-AuNPs	29.1	-49.9	38
Buffer-AHMP-AuNPs	27.6	-58.2	35
calcium-Buffer-AHMP-AuNPs	65.4	-50.3	26

2.2 Colorimetric assay of calcium

Following the AuNPs modification, a colorimetric analysis using AHMP-AuNPs was performed for the detection of calcium. The color and absorption spectra of the AHMP-AuNPs with and without calcium are shown in Figure 24 while their zeta potential was displayed in Table 5. After addition of buffer, the negative charge of AHMP-AuNPs solution increased from -49.9 mV to -58.2 mV, while the average size of the buffer-AHMP-AuNPs was not significantly change (from 29.1 to 27.6 nm). After addition of calcium, the zeta potential dramatically decreased from -58.2 mv, intensity 35 a.u., to -50.3 mv, intensity 26 a.u., while the average size of the AHMP-AuNPs increased from 29.1 to 65.4 nm. These results indicate that the AHMP-AuNPs aggregation was induced by the electrostatic force between the positive charge of calcium and the negative charge of AHMP-AuNPs. Moreover, the results obtained corresponded to the decrease of the absorption bands at 273 and 523 nm along with the formation of a new absorption band at 680 nm (redshift), as illustrated in Figure 24. Furthermore, the color of the AHMP-AuNPs on the proposed device was clearly observed to change from red to blue immediately, which suggested the growth of the nanoparticles' size. This indicates that calcium could quickly bind to their functional groups (–NH2 and –OH) onto modified

AuNPs. These binding interactions and electrostatic force all contribute to the aggregation mechanism of the AuNPs, as schematically illustrated in Figure 25. According to the considerable change in negative charge, color and LSPR absorption of AHMP-AuNPs upon the addition of calcium, the development of a novel colorimetric AHMP-AuNPs device for calcium determination was successfully accomplished.
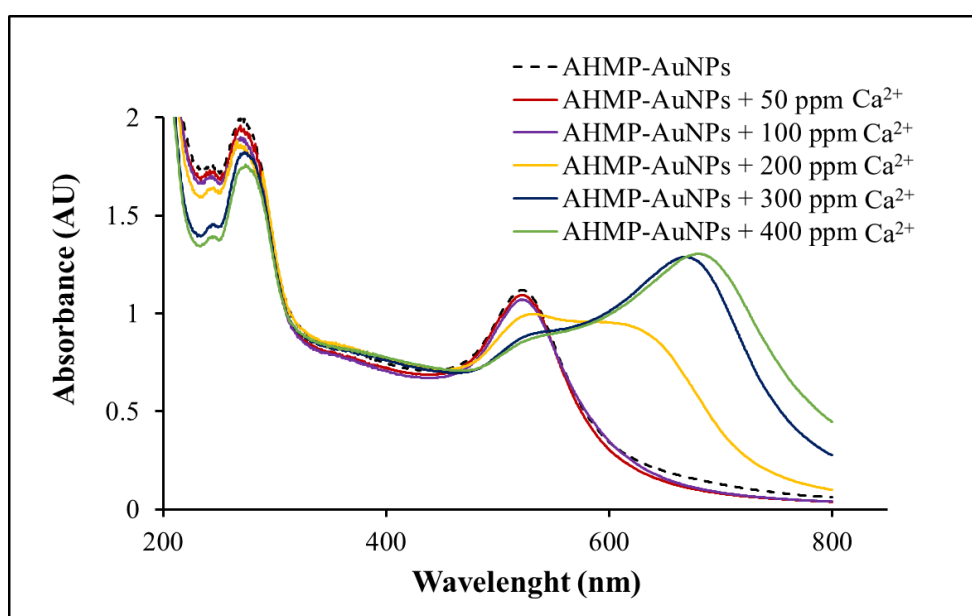
Figure 24 UV- Vis absorption spectra of AHMP-AuNPs (dot line) and AHMP-AuNPs in the presence of calcium at 50 (red line), 100 (purple line), 200 (yellow line), 300 (navy-blue line) and 400 ppm (green line).
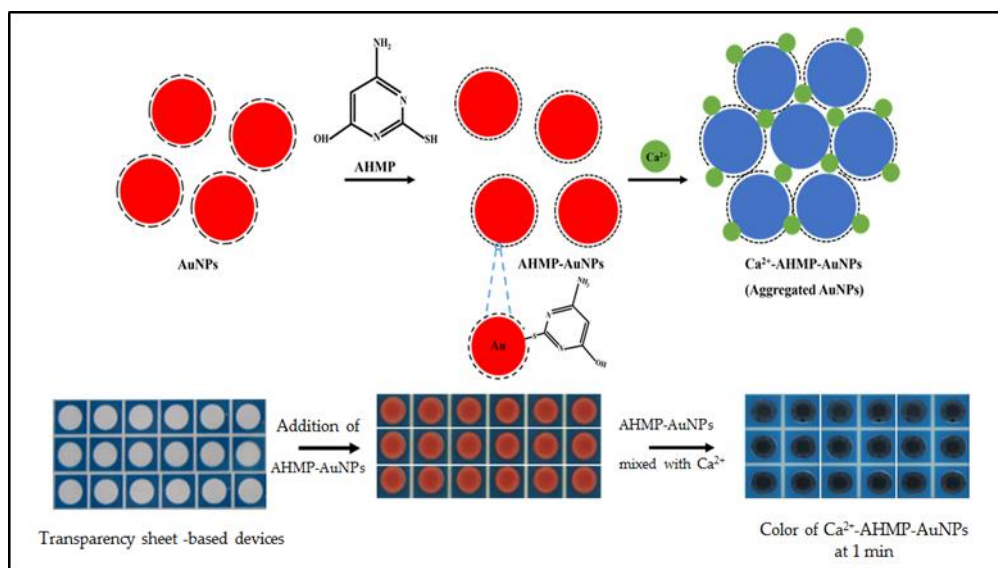
Figure 25 Mechanism scheme of AHMP-AuNPs for colorimetric detection of calcium. AHMP was modified onto the surface of AuNPs and increased in size because AuNPs could be aggregated via electrostatic force between AHMP-AuNPs and calcium. The color changed from red to blue in accordance with the size of AuNPs.

2.3 Optimization condition for analysis calcium

In this section, the modifier volume ratio, pH, the incubation time and AHMP-AuNPs: sample volume ratios were examined for optimization parameters. The colorimetric detection of calcium was performed at room temperature by dropping sequentially of standard calcium and AHMP-AuNPs on the detection zone of transparency sheets. The red/blue intensity was measured and calculated by mobile phone and image J software, respectively. The resulting of aggregation capability between AHMP-AuNPs and calcium in each condition was observed with the red/blue intensity form transparency sheet image. First, the volume of 4mM AHMP modifier was varied in the range of 0.1, 0.2, 0.4, 0.6, 0.8, 1.0, 1.2 and 1.5 mL at the same concentered AuNPs volume (1.5 mL). Then, 15 µL of the varied AHMP-AuNPs were investigated with 15 µL of calcium at 0, 10, 50 and 100 ppm concentration, respectively. In Figure 26, the red/blue intensity of blank (AHMP-AuNPs and PBS Buffer pH6) was

decreased when the AHMP volumes were increased. Volumes were increased. It may be that the AuNPs were diluted by the AHMP solution, so that AHMP-AuNPs had reduced aggregation efficiency. The red/blue intensity of 0.1 mL AHMP was found to exhibit the most significant change from the blank, especially when tested with 100 ppm calcium. Moreover, this change could be easily detected with the naked eye. Therefore, 0.1 mL AHMP was selected as an optimum modifier volume for further studies.
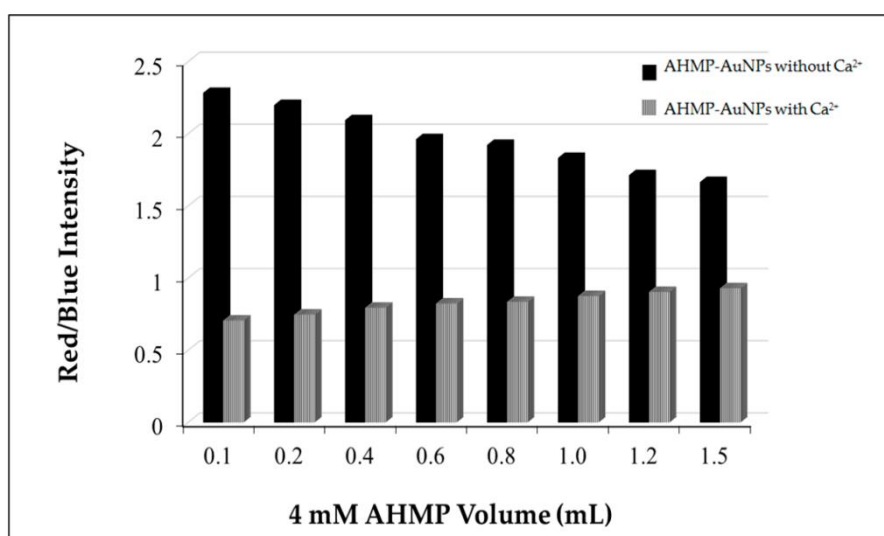
Figure 26 The red/blue intensity of the AHMP-AuNPs at different AHMP volume at 0.1, 0.2, 0.4, 0.6, 0.8, 1.0, 1.2 and 1.5 mL without (solid bar) and with (thin bar) calcium at 100 ppm.

Then, the effect of pH (range of 3–12) on the aggregation process was studied. As shown in Figure 27, the use of phosphate buffer with pH of 5.8–12 did not change the color of the blank. Therefore, phosphate buffers of pH 5.8–12 were chosen to study the aggregation effect of AHMP-AuNPs and 100 ppm calcium at a 1:1 volume ratio. The results demonstrated that pH 6 provided the maximum color change. At this pH, calcium has a high potential to induce the aggregation of AHMP-AuNPs. Therefore, phosphate buffer pH 6 was chosen for further studies.
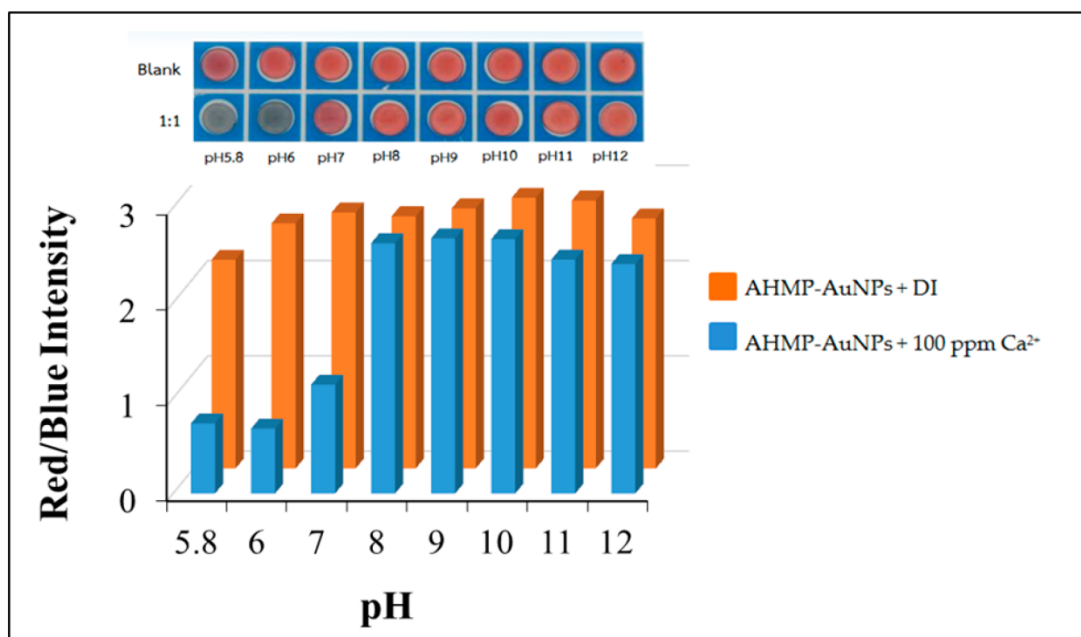
Figure 27 The influence of pH over the range 5.8-12 on the aggregation process of the AHMP-AuNPs and 100 ppm calcium.

Next, the aggregation of AHMP-AuNPs induced by calcium was investigated at various incubation times (1 – 30 min). The aggregation of the AHMP-AuNPs occurred immediately after the addition of calcium, and was completed in 1 minute. In other words, the red/blue intensity from the aggregation of AHMP-AuNPs induced by calcium can be measured at 1 minute. When AHMP-AuNPs were left on the device for over 5 minutes, the red/blue intensity of the blank was increased from the initial (Figure 28) because of self-aggregation of the AHMP-AuNPs. In the case of interferences, Mg^{2+} was first selected as a representative of other positive ions, as it has an atomic radius and positive charge nearly equal to those of calcium to investigate the possibility of using this proposed probe. From these results, it was found that the red/blue intensity of AHMP-AuNPs in the presence of Mg^{2+} were decreased more than 5%, compared to the blank, after 5 minutes. This indicated that other positive ions may also interfere with the proposed method if the incubation time was over 5 minutes. From this critical observation, we strongly believed that an incubation time of 1 minute is appropriate to

specify the detection of calcium by electrostatic force and size selective in the presence of others divalent ions. Therefore, the incubation time is critical point that has to keep in mind for selectivity study in the following part.
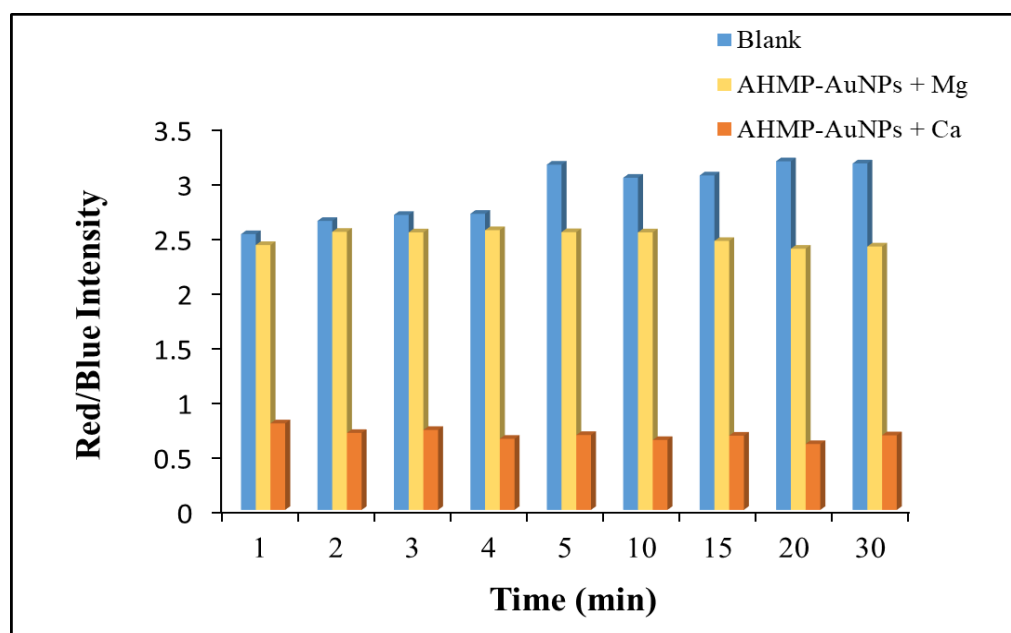
Figure 28 Effects of the incubation time for the aggregation of AHMP-AuNPs without and with calcium 100 ppm compare with Mg^{2+} 100 ppm, phosphate buffer pH 6, AHMP-AuNP: sample volume ratio at 1:1

Finally, to find a suitable quantity of the AHMP-AuNPs that can sufficiently interact with calcium, the reagent volume ratio was tested between 5:25 - 25:5. The red/blue intensity of AHMP-AuNPs after the mixing of calcium was measured at various reaction volume ratios with 30 µL maximum drop volume. As shown in Figure 29, the volume ratio of AHMP-AuNPs: calcium at 25:5 was indicated the highest red/blue intensity. It had shown that 25:5 of AHMP-AuNPs: calcium was sufficient and appropriate with calcium solution in our proposed method.
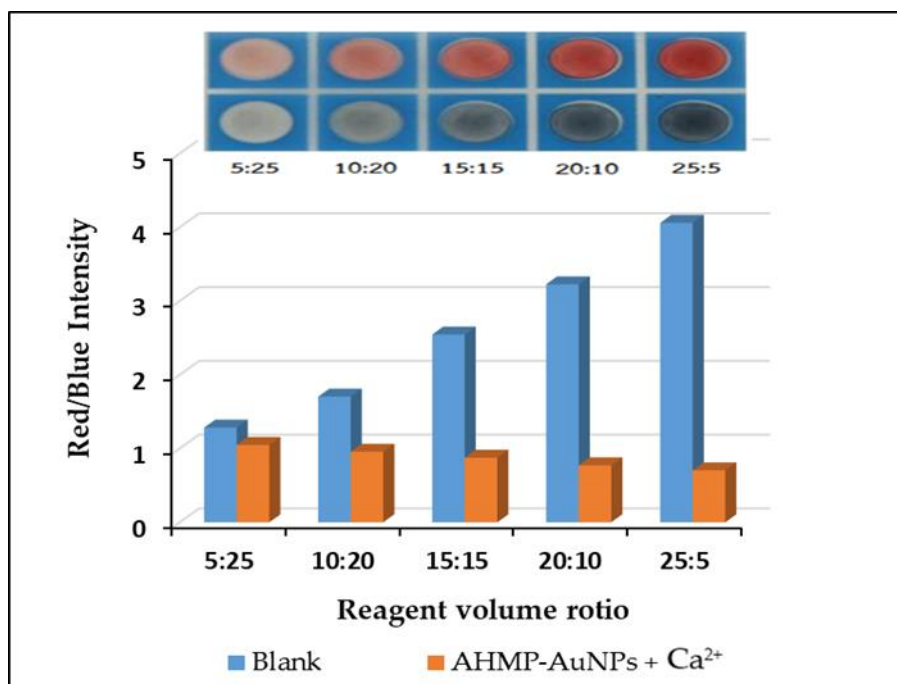
Figure 29 Effects of the reagent volume ratio for the aggregation of AHMP-AuNPs and calcium at 100 ppm, incubation time of 1 minute and other conditions used as same as optimal values.

2.4 Selective determination of calcium

After obtaining the optimal conditions, selectivity was evaluated by the Δred/blue intensity (red/blue intensity of blank – red/blue intensity of sample) of AHMP-AuNPs mixed with other substances and metal ions possibly found in urine, i.e., ascorbic acid, uric acid, albumin, glucose, Mg^{2+}, K^+, Na^+, Cl^-, CO_3^-, PO_4^{2-} and SO_4^{2-}, since they may also affect the aggregation of AHMP-AuNPs and might interfere with the method accuracy. An interference was defined to happen when the Δred/blue intensity in the mixture varied by more than ±5% of the calcium intensity. As emphasized previously, the incubation time directly affects to the selectivity. Therefore, the change of color was measured at 1 minute after mixing to neglect the interference from Mg^{2+}. As shown in Figure 30, the results demonstrated clearly that the Δred/blue intensity of AHMP-AuNPs mixed with foreign compounds with concentrations even 10 times greater

than the concentration of calcium did not significantly affect the signal of calcium. In addition, we also applied this probe for detection of other divalent cations such as Hg^{2+}, Cu^{2+}, Cd^{2+} and Zn^{2+}. According to the results, it can be seen that the interferences from almost all metal ions studied did not affect calcium detection. Therefore, this probe provides high selectivity for only calcium detection at incubation time of 1 minute.
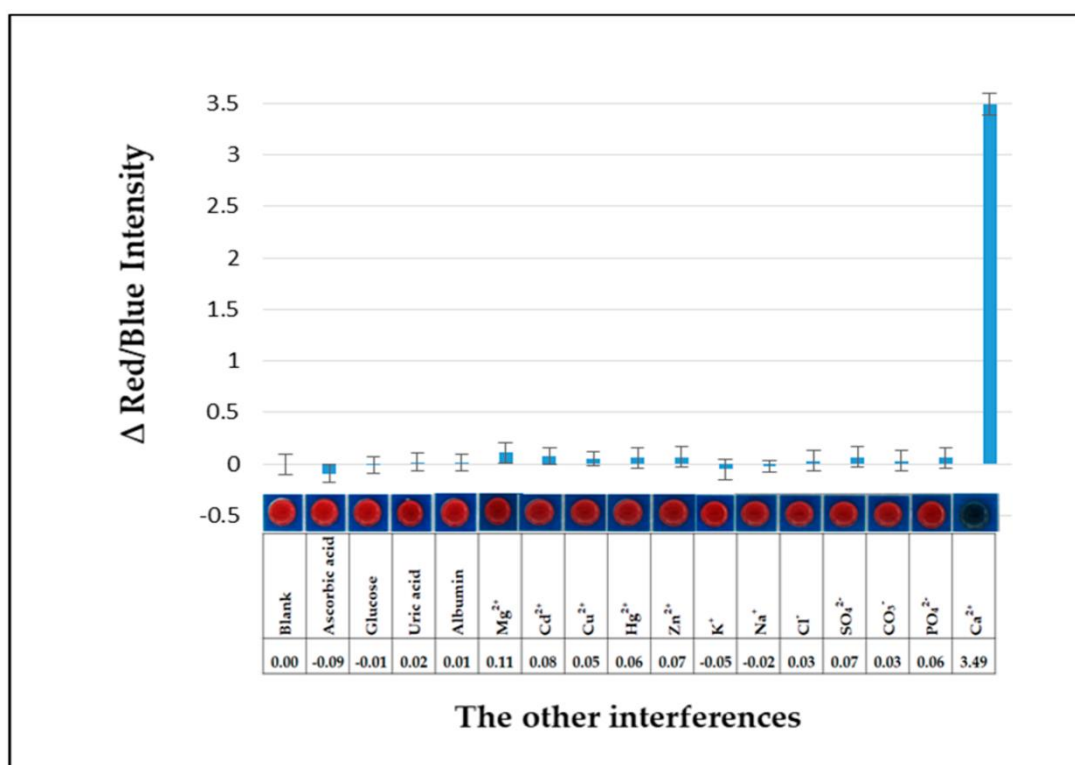
Figure 30 Responses of AHMP-AuNPs in the other interferences. The concentration of calcium was fixed at 100 ppm while other interferences were used at 1,000 ppm. All results were repeated three times (n=3). Other conditions were used as same as optimal values.

2.5 Analytical performances

The proposed method was investigated in the aggregation of AHMP-AuNPs and calcium on transparency sheet-base device. Calcium was studied between 0 and 100 ppm using the optimum conditions. As shown in Figure 31, it was found that the Δred/blue intensity from the aggregation of AHMP-AuNPs and calcium were significantly reduced while the concentrations of calcium were increased. A linear relationship between the red/blue intensity and Log of calcium concentration in the calibration curve was established. A good linearity was observed for the concentration of calcium range from 10 ppm to 100 ppm with the correlation coefficient of 0.9877. The limit of detection and limit of quantitation for calcium were found to be 3.05 ppm and 10.17 ppm (N=3), respectively.
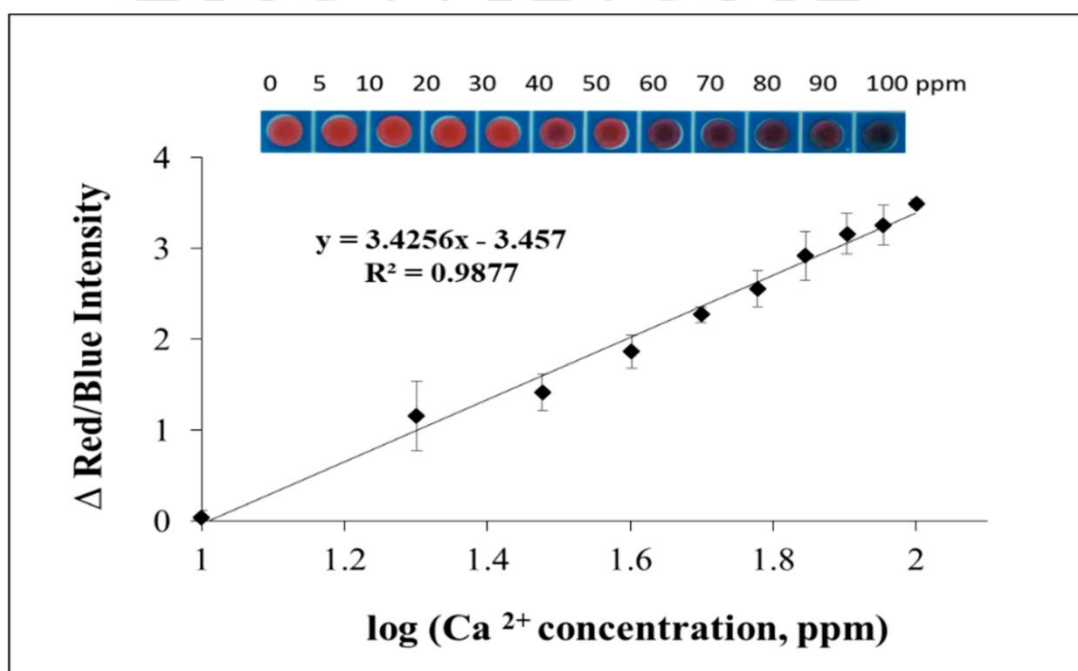
Figure 31 The transparency sheet-based devices for the quantitative analysis of calcium and the calibration plot of Δred/blue intensity and the log concentration of calcium (error bar represented the standard deviation at n = 3). Other conditions were used as same as optimal values.

2.6 Analysis of real samples and method validation

To evaluate the efficiency of the proposed method, the transparency sheet-based device was used to detect calcium in urine samples, and the results were compared with AAS. The urine samples were spiked with the standard calcium at 80, 160 and 320 ppm. Then, the samples were further diluted to produce a final appropriate dilution factor before analysis. All urine samples were also analyzed by AAS standard method and the proposed method. The obtained concentrations from two methods were statistically compared using T- test. T-test calculation was obtained the value at 1.75 which lower than $t_{Critical}$ = 4.30. So, there was no significant difference between the concentrations obtained from the two methods. The proposed method has a good recovery in the range of 103.69 - 104.25%. These recoveries were within the acceptable recovery percentages, 95–105 % for a concentration of 0.1% (w/v) or at the calcium concentration lower than 1,000 ppm recommended by the Association of Official Analytical Chemists (AOAC). As the results, this proposed colorimetric method can be applied for the calcium determination of the urine sample with satisfactory results.

CHAPTER V

CONCLUSION AND FUTURE DIRECTIONS

1. Summary of work

Colorimetric methods using gold nanoparticles (AuNPs) for the determination of vitamin B1 and calcium in urine have been extensively used in this present. The objective of this work was to develop, determine the optimum conditions, and to apply transparency sheet-based analytical devices for the detection of vitamin B1 or calcium in urine. From the results, they were successfully demonstrated that colorimetric methods using AuNPs can detect vitamin B1 and calcium in urine samples.

1.1 Colorimetric determination of vitamin B1 in urine samples using gold nanoparticles (AuNPs) sensing

The use of AuNPs for the colorimetric sensing of vitamin B1 in transparency sheet-based devices is to provide rapid, easy to use, inexpensive, and portable devices for point-of-care monitoring. The sensor based on the aggregation of AuNPs on a transparency sheet substrate by the strong affinity and electrostatic force between AuNPs and vitamin B1, which leads to a shift in the absorption spectrum. Furthermore, the other vitamin species and common interfering molecules have no appreciable change. Except for the concentration of vitamin B2, vitamin B6 and vitamin B12 over 100 ppb were interfered this method. Anyway, in urine sample, the concentration of vitamin B2, vitamin B6 and vitamin B12 were lower than 100 ppb. The achieved experimental high selectivity and sensitivity is owing to strong electrostatic interactions between positively charged from vitamin B1 and negatively charged from AuNPs. For quantitative measurement, a good linear relationship (R^2 = 0.9913) between vitamin B1 concentration and average mean red intensity was obtained in the range of 40-200 ppb. The limit of detection (LOD) and the limit of quantitation (LOQ) for vitamin B1 were found to be 3.00 ppb and 10.01 ppb, respectively. Finally, our transparency sheet-based devices were successfully applied to the semi-quantitative analysis of

vitamin B1 in urine samples. Then, the transparency sheet-based devices would be potentially modified with AuNPs for the detection of a variety of other targets.

1.2 Colorimetric determination of calcium in urine samples using AHMP-modified gold nanoparticles (AuNPs)

In summary, this work was demonstrated the first time using AHMP modified AuNPs for colorimetric method on transparency sheet-based device to provide simple, rapid, inexpensive and portable devices for calcium determination. This method was based on the aggregation of AHMP-AuNPs on the transparency sheet-based by the electrostatic force between negative charge of AHMP-AuNPs and positive charge of calcium. Under optimal condition, the color change of AHMP-AuNPs can be observable by the naked eye. The calibration curve of calcium was linear and in the range of 10-100 ppm (R^2 as a linear relationship = 0.9877). The limit of detection (LOD) and the limit of quantitation (LOQ) were found to be 3.05 ppm and 10.17 ppm, respectively. Furthermore, the proposed method was successfully applied to the quantitative analysis of calcium in urine sample. The devices would be potentially AuNPs-modified with AHMP for the detection of a variety of other metal ion. This colorimetric device provided a result within 1 minute that was much faster than other methods. This simple device is very suitable for calcium quantitative analysis which use as an alternative method for the rapid screening of calcium deficiency with no need for any special instrument.

2. Future Directions

This work has been successfully applied for the determination of vitamin B1 and calcium in urine samples by colorimetric methods using gold nanoparticles (AuNPs). The proposed methods showed rapid and simple procedures. However, the pre-concentrated AuNPs and AHMP-AuNPs are limited to merely research and developing. Further researches should consider fully apply these technologies to industrial fields, and particularly for the biomarker. This developed method is a part of model for creating other analytical devices in the future.

REFERENCES

Abdou, E., & Hazell, A. S. (2015). Thiamine deficiency: an update of pathophysiologic mechanisms and future therapeutic considerations. *Neurochem Res, 40*(2), 353-361. doi: 10.1007/s11064-014-1430-z

Ahmed, M., Azizi-Namini, P., Yan, A. T., & Keith, M. (2015). Thiamin deficiency and heart failure: the current knowledge and gaps in literature. *Heart Fail Rev, 20*(1), 1-11. doi: 10.1007/s10741-014-9432-0

Allison, M. G., & McCurdy, M. T. (2014). Alcoholic metabolic emergencies. *Emerg Med Clin North Am, 32*(2), 293-301. doi: 10.1016/j.emc.2013.12.002

Apilux, A., Dungchai, W., Siangproh, W., Praphairaksit, N., Henry, C. S., & Chailapakul, O. (2010). Lab-on-paper with dual electrochemical/colorimetric detection for simultaneous determination of gold and iron. *Anal Chem, 82*(5), 1727-1732. doi: 10.1021/ac9022555

Armbrecht, M. (2011). Generation of a standard curve for a colorimetric assay in the eppendorf BioSpectrometer® basic and Eppendorf BioSpectrometer® kinetic, User guide. *Eppendorf AG*, 1-6.

Baraa, M. (2015). Gold nanoparticles for determination of biomolecules. Retrieved from http://www.slideshare.net/Albairaq/presentation-al-bairaq-repaired

Batifoulier, F., Verny, M. A., Besson, C., Demigne, C., & Remesy, C. (2005). Determination of thiamine and its phosphate esters in rat tissues analyzed as thiochromes on a RP-amide C16 column. *J Chromatogr B Analyt Technol Biomed Life Sci, 816*(1-2), 67-72. doi: 10.1016/j.jchromb.2004.11.004

Brown, P. (2000). Colorimetry-Quantitative Analysis and Determining the Formula of a Complex ion.   http://www.docbrown.info/page07/appendixtrans09.htm

Carrie, E. B., Richard L. Berg, & Urquhart, A. C. (2014). 24-Hour urinary calcium in primary hyperparathyroidism. *Clinical Medicine & Research, 11*(4), 219-225. doi: 10.3121/cmr.2013.1164

Chen, Y., Xianyu, Y., & Jiang, X. (2017). Surface Modification of Gold Nanoparticles with Small Molecules for Biochemical Analysis. *Acc Chem Res, 50*(2), 310-319. doi: 10.1021/acs.accounts.6b00506

Clark, J. (2015). The Beer-Lambert Law. Retrieved from
http://chemwiki.ucdavis.edu/Core/Physical_Chemistry/Spectroscopy/Electronic_
Spectroscopy/Electronic_Spectroscopy_Basics/The_Beer-Lambert_Law

Council, N. R. (1989). Recommended Dietary Allowances, 10th ed. *Washington D.C.,
National Academy York Academy Press*.

Densupsoontorn, N., Jirapinyo, P., & Kangwanpornsiri, C. (2013). Micronutrient
deficiencies in obese Thai children. *Asia Pac J Clin Nutr, 22*(3), 497-503. doi:
10.6133/apjcn.2013.22.3.06

Edwards, K. A., Tu-Maung, N., Cheng, K., Wang, B., Baeumner, A. J., & Kraft, C. E.
(2017). Thiamine Assays-Advances, Challenges, and Caveats. *ChemistryOpen,
6*(2), 178-191. doi: 10.1002/open.201600160

Elghanian, R., Storhoff, J. J., Mucic, R. C., Letsinger, R. L., & Mirkin, C. A. (1997).
Selective colorimetric detection of polynucleotides based on the distance-
dependent optical properties of gold nanoparticles. *Science, 277*(5329), 1078-
1081.

Ferreira, T., & Rasband, W. (2012). ImageJ User Guide.
http://imagej.nih.gov/ij/docs/guide

Gafni, R. I., Guthrie, L. C., Kelly, M. H., Brillante, B. A., Christie, C. M., Reynolds, J. C.,
Collins, M. T. (2015). Transient Increased Calcium and Calcitriol Requirements
After Discontinuation of Human Synthetic Parathyroid Hormone 1-34 (hPTH 1-34)
Replacement Therapy in Hypoparathyroidism. *J Bone Miner Res, 30*(11), 2112-
2118. doi: 10.1002/jbmr.2555

Grasseschi, D., Zamarion, V. M., Araki, K., & Toma, H. E. (2010). Surface enhanced
Raman scattering spot tests: a new insight on Feigl's analysis using gold
nanoparticles. *Anal Chem, 82*(22), 9146-9149. doi: 10.1021/ac102238f

Group, F. W. E. (1962). Calcium requirements, Food and Agriculture Organization of the
United Nations. *FAO Nutrition Meetings Report Series, No. 30*.

Havezov, I. (1996). Atomic absorption spectrometry (AAS) - a versatile and selective detector for trace element speciation. *Anal Bioanal Chem, 355*(5-6), 452-456. doi: 10.1007/s0021663550452

Hinterwirth, H., Wiedmer, S. K., Moilanen, M., Lehner, A., Allmaier, G., Waitz, T., Lammerhofer, M. (2013). Comparative method evaluation for size and size-distribution analysis of gold nanoparticles. *J Sep Sci, 36*(17), 2952-2961. doi: 10.1002/jssc.201300460

Homola, J., Yee, S. S., & Gauglitz, G. (1999). Surface Plasmon Resonance Sensors: Review. *Sensors and Actuators B: Chemical, 54*, 3-15.

Hyperparathyroidism, A. A. T. F. O. P. (2005). The American Association of Clinical Endocrinologists and the American Association of Endocrine Surgeons position statement on the diagnosis and management of primary hyperparathyroidism. *Endocr Pract, 11*, 49-54.

Ito, Y., Yamanaka, K., Susaki, H., & Igata, A. (2012). A cross-investigation between thiamin deficiency and the physical condition of elderly people who require nursing care. *J Nutr Sci Vitaminol (Tokyo), 58*(3), 210-216.

Jansen, B. C. P. (1936). A chemical determination of aneurin (= vitamin B1) by the thiochrome reaction. *Recueil des Travaux Chimiques des Pays-Bas, 55*(12), 1046-1052. doi: https://doi.org/10.1002/recl.19360551211

Jenco, J., Krcmova, L. K., Solichova, D., & Solich, P. (2017). Recent trends in determination of thiamine and its derivatives in clinical practice. *J Chromatogr A, 1510*, 1-12. doi: 10.1016/j.chroma.2017.06.048

Kamruzzaman, M., Alam, A. M., Lee, S. H., & Dang, T. D. (2013). Chemiluminescence microfluidic system on a chip to determine vitamin B1 using platinum nanoparticles triggered luminol–$AgNO_3$ reaction. *Sens. Actuators. B., 185*, 301-308.

Karita, S., & Kaneta, T. (2016). Chelate titrations of Ca(2+) and Mg(2+) using microfluidic paper-based analytical devices. *Anal Chim Acta, 924*, 60-67. doi: 10.1016/j.aca.2016.04.019

Kerns, J. C., Arundel, C., & Chawla, L. S. (2015). Thiamin deficiency in people with obesity. *Adv Nutr, 6*(2), 147-153. doi: 10.3945/an.114.007526

Kraut J, & J, R. H. (1962). The crystal structure of thiamine hydrochloride (vitamin B). *Acta Crystallogr., 15*, 747-757.

Lee, B. Y., Yanamandra, K., & Bocchini, J. A., Jr. (2005). Thiamin deficiency: a possible major cause of some tumors? (review). *Oncol Rep, 14*(6), 1589-1592.

Lerga, T. M., & O'Sullivan, O. S. (2008). Rapid determination of total hardness in water using fluorescent molecular aptamer beacon. *Anal Chim Acta., 610*(1), 105-111. doi: doi: 10.1016/j.aca.2008.01.031.

Liddicoat, C., Hucker, B., Liang, H., & Vriesekoop, F. (2015). Thiamin analysis in red wine by fluorescence reverse phase-HPLC. *Food Chem, 177*, 325-329. doi: 10.1016/j.foodchem.2015.01.009

Lonsdale, D. (2006). A review of the biochemistry, metabolism and clinical benefits of thiamin(e) and its derivatives. *Evid Based Complement Alternat Med, 3*(1), 49-59. doi: 10.1093/ecam/nek009

Lopez-Molinero, A., Tejedor Cubero, V., Domingo Irigoyen, R., & Sipiera Piazuelo, D. (2013). Feasibility of digital image colorimetry--application for water calcium hardness determination.*Talanta, 103*, 236-244. doi: 10.1016/j.talanta.2012.10.038

Losa, R., Sierra, M. I., Fernandez, A., Blanco, D., & Buesa, J. M. (2005). Determination of thiamine and its phosphorylated forms in human plasma, erythrocytes and urine by HPLC and fluorescence detection: a preliminary study on cancer patients. *J Pharm Biomed Anal, 37*(5), 1025-1029. doi: 10.1016/j.jpba.2004.08.038

Lu, J., & Frank, E. L. (2008). Rapid HPLC measurement of thiamine and its phosphate esters in whole blood. *Clin Chem, 54*(5), 901-906. doi: 10.1373/clinchem.2007.099077

Macek, T. J., Feller, B. A., & Hanus, E. J. (1950). Pharmaceutical studies with thiamine mononitrate. *J Am Pharm Assoc Am Pharm Assoc, 39*(7), 365-369.

Maryam, A. O., Akram, H., & Heidari, T. (2017). A novel direct and cost effective method for fabricating paper-based microfluidic device by commercial eye pencil and its application for determining simultaneous calcium and magnesium. *Microchemical Journal, 133*, 545-550. doi: https://doi.org/10.1016/j.microc.2017.04.031

McCabe, B. J. (2004). Prevention of food-drug interactions with special emphasis on older adults. *Curr Opin Clin Nutr Metab Care, 7*(1), 21-26.

Nanocomposix. (2012). *Zeta potential analysis of nanoparticals* Vol. 1.1. Retrieved from Nanocomposix.com

Molina-Delgado, M. A., Aguilar-Caballos, M. P., & Gómez-Hens, A. (2016). Simultaneous photometric microplate assay for free and total thiamine using gold nanoparticles and alkaline phosphatase. *Microchim. Acta., 183*, 1385–1390.

Neouze, M. A., & Schubert, U. (2008). Surface Modification and Functionalization of Metal and Metal Oxide Nanoparticles by Organic Ligands. *Monatshefte für Chemie - Chemical Monthly, 139*(3), 183-195.

Nilapwar, S. M., Nardelli, M., Westerhoff, H. V., & Verma, M. (2011). Absorption spectroscopy. *Methods Enzymol, 500*, 59-75. doi: 10.1016/B978-0-12-385118-5.00004-9

Okamoto, T., Yamaguchi, I., & Kobayashi, T. (2000). Local plasmon sensor with gold colloid monolayers deposited upon glass substrates. *Opt Lett, 25*(6), 372-374.

Organization, W. H. (1998). Joint FAO/WHO Expert Consultation on Human Vitamin and Mineral Requirements(1998 : Bangkok, Thailand). *report of a joint FAO/WHO expertconsultation, Bangkok, Thailand, 21–30 September 1998.*

Penner, M. H. (2010). *Basic Principles of Spectroscopy , Food analysis* (Fourth ed.): Springer.

Qi, W., Zhong-Fang, L., Ling, K., & Liu, S. P. (2007). Absorption and Resonance Rayleigh Scattering Spectra of the Interaction for Copper Nanoparticles with Vitamin B1. *Chinese Journal of Analytical Chemistry, 35*(3), 365-369. doi: doi.org/10.1016/S1872-2040(07)60040-1

Rajamanikandan, R., & Ilanchelian, M. (2017). Simple and visual approach for highly selective biosensing of vitaminB1 based on glutathione coated silver nanoparticles as a colorimetric probe. *Sens. Actuators. B., 244*, 380-386.

Rahman, S. T. A., Elbashir, A. A., El-Mukhtar, M., & Ibrahim, M. M. (2016). Application of Spectrophotometric Methods for the Determination of Thiamine (VB1) in Pharmaceutical Formulations Using 7-Chloro-4-Nitrobenzoxadiazole (NBD-Cl) *Analytical & Pharmaceutical Research, 2*(3), 1-6.

Sauberlich, H. E. (1967). Biochemical alterations in thiamine deficiency - their interpretation. *American Journal of Clinical Nutrition, 20*, 528-546.

Shankar, S., & John, S. A. (2015). Sensitive and highly selective determination of vitamin B1 in the presence of other vitamin B complexes using functionalized gold nanoparticles as fluorophore. *RSC Adv., 5*, 49920–49925.

Sergeev, G. B., & Shabatina, T.I. (2002). Low temperature. Surface chemistry and nanostructures. *Surf. Sci., 500*, 628-655.

Sethi, M., & Knecht, M. R. (2010). Understanding the mechanism of amino acid-based Au nanoparticle chain formation. *Langmuir, 26*(12), 9860-9874. doi: 10.1021/la100216w

Subodh, K. (2006). *Spectroscopy of Organic Compounds*. Department of Chemistry Guru Nanak Dev University.

Tan, H., Li, Q., Zhou, Z., Ma, C., Song, Y., Xu, F., & Wang, L. (2015). A sensitive fluorescent assay for thiamine based on metal-organic frameworks with intrinsic peroxidase-like activity. *Anal Chim Acta, 856*, 90-95. doi: 10.1016/j.aca.2014.11.026

Tsien, R. Y. (1980). New calcium indicators and buffers with high selectivity against magnesium and protons: design, synthesis, and properties of prototype structures. Biochemistry., 19(11), 2396-2404.

Waheed, P., Naveed, A. K., & Ahmed, T. (2013). Thiamine deficiency and its correlation with dyslipidaemia in diabetics with microalbuminuria. *J Pak Med Assoc, 63*(3), 340-345.

Yu, J., Zhang, X., Lu, Q., Wang, X., Sun, D., Wang, Y., & Yang, W. (2017). Determination of calcium and zinc in gluconates oral solution and blood samples by liquid cathode glow discharge-atomic emission spectrometry. *Talanta, 175*, 150-157. doi: 10.1016/j.talanta.2017.07.040

Zhou, Z., Tan, C., Zheng, Y., & Wang, Q. (2013). Electrochemical signal response for vitamin B1 using terbiumluminescent nanoscale building blocks as optical sensors. *Sens. Actuators. B., 188*, 1176– 1182.

VITA

NAME	Miss Paweenar Duenchay
DATE OF BIRTH	13 April 1980
PLACE OF BIRTH	Prachin Buri
INSTITUTIONS ATTENDED	High School Graduation
	Benjamaracharangsarit School, 1999
	Bachelor of Engineering (Chemical Engineering)
	Suranaree University of Technology, 2003
	Master of Engineering (Chemical Engineering)
	Chulalongkorn University, 2006
HOME ADDRESS	1316/15 Soi Lat Phrao 41/1, Samsen Nok, Huai Khwang,
	Bangkok 10310
PUBLICATION	- Duenchay P;, Chailapakul O.; Siangproh W.; "A Transparency Sheet-Based Colorimetric Device for Simple Determination of Calcium Ions Using Induced Aggregation of Modified Gold Nanoparticles" Int. J. Mol. Sci. 2019, 20, 2954; doi:10.3390/ijms20122954.